Linköping Studies in Science and Technology
Dissertation No. 1142

Electronic Transport in Polymeric Solar Cells and Transistors

Lars Mattias Andersson

Linköping University
INSTITUTE OF TECHNOLOGY

Biomolecular and Organic Electronics
Department of Physics, Chemistry and Biology
Linköpings universitet, SE-581 83 Linköping, Sweden

Linköping 2007

ISBN 978-91-85895-50-2
ISSN 0345-7524

Printed by LiU-Tryck, Linköping 2007

Abstract

The main topic of this dissertation is electronic charge transport in polymeric and molecular organic materials and material blends intended for solar cell applications. Charge transport in polymers is a strange beast and carrier mobility is rarely a well-defined number. Measurements on different sample geometries and under different conditions tend to give different results and when everything is to be related to solar cell performance it is imperative that there is a way to correlate the results from different measurements. Polymer solar cells utilize composite materials for their function. This puts an additional twist on charge transport studies, as there will also be interaction between the different phases to take into account.

Several measurement techniques have been used and their interrelationships as well as information on their relevance for solar cells have been investigated. Field effect transistors (FET) with an organic active layer have proved to be one of the more versatile measurement geometries and are also an interesting topic in itself. FETs are discussed both as a route for material characterization and as components. A main result correlates bias stress in organic field effect transistors with the electronic structure of the material.

Power conversion efficiency in solar cells is discussed with respect to electrical properties. The interaction of different blend materials and the impact of stoichiometry on transport properties in the active layer have been investigated. Results indicate that charge transport properties frequently are a key determining factor for which material combinations and ratios that works best.

Some work on the conductive properties of nano-fibers coated with semiconducting polymers has also been done and is briefly discussed. The conductive properties of nano-fibers have been studied through potential imaging.

Populärvetenskaplig sammanfattning

Organisk elektronik är ett område där de ofta mycket väldefinerade oorganiska halvledarna har ersatts med kolbaserade polymerer och molekyler som oftast är relativt oordnade. I princip alla traditionella halvledarfunktioner är möjliga att realisera med organiska komponenter, men deras mer varierade natur medför att det finns en stor mängd fysikaliska skillnader. Generellt sett så är prestanda sämre hos en organisk komponent än för motsvarande oorganiska, men faktorer såsom pris, produktionsmetoder, miljöbelastning och inte minst det faktum att komponenterna kan göras flexibla, talar för att det kommer att finnas utrymme för organisk elekronik i ett flertal applikationer inom de närmaste åren. Ett exempel på en redan kommersialiserad tillämpning är i bildskärmar, där hybridteknologi inom en snar framtid kan komma att leverera bättre prestanda än sina helt oorganiska motsvarigheter. I en sådan bildskärm injiceras hål och elektroner i det organiska materialet, där de sedan rekombinerar och skickar ut ljus med en färg som bestäms av den elektroniska strukturen hos materialet. Den omvända processen, där ljus omvandlas till elektricitet är också möjligt och det är mycket liten skillnad på komponentstrukturen. Prestanda hos komponenterna är i stor utsträckning beroende av laddningstransporten.

Det som kännetecknar en organisk halvledare är det konjugerade kolskelettet, där kolatomerna binder till varandra med ömsom enkel- och ömsom dubbelbindningar. Elektronerna i dubbelbindningarna är relativt löst associerade med en specifik kolatom och kan med små medel förmås att flytta på sig. Den inneboende oordningen i organiska halvledare medför dock att mekanismerna för denna laddningstransport på många väsentliga punkter skiljer sig från den i välordnade oorganiska material. Laddningstransporten går att undersöka på många olika sätt. Man kan studera laddningarna direkt, genom extraktions- eller förskjutningsströmmar, eller också kan man bygga komponenter och studera deras prestanda utifrån givna modeller.

Organiska solceller baseras på ett aktivt lager bestående av en blandning av två

olika material med olika elektronaffinitet, ofta en polymer och en fulleren, som placeras mellan två olika elektroder. Ljus absorberas i det aktiva lagret och genererar ett bundet laddningspar som separeras i gränsytan mellan polymeren och fullerenen. De fria laddningarna transporteras därefter ut till elektroderna med hjälp av det elektriska fält som uppkommer på grund av komponentens asymmetri. På sin väg ut mot elektroderna kan laddningarna gå förlorade genom rekombination. Den hastighet med vilken de färdas måste således vara stor nog för att de skall hinna fram till eletroderna innan rekombination sker. Hastigheten, mobiliteten, hos laddningsbärare i relevanta materialkombinationer har studerats med hjälp av extraktionsströmmar och fälteffekttransistorer. Resultaten visar att det föreligger avsevärda mobilitetsskillnader mellan olika material och att mobiliteterna är beroende av vilka material som blandas och dess mängdförhållande. En direkt korrelation mellan transportegenskaper och solcellsprestanda föreligger också, vilket indikerar att laddningstransporten är för långsam och att rekombination förhindrar samtliga genererade laddningsbärare från att utvinnas som elektricitet.

Preface

A constant and growing need for humanity is energy. The demand is virtually limitless but the supply, in a useful state, is not. Energy in general is abundant. Every year, solar irradiation on the order of $1000kWh/m^2$ hits the surface of the earth and to harness that energy would be immensely useful. Solar cells are a very viable option for this but many the existing technologies have a very long energy payback time high cost. Polymer based devices does not suffer these drawbacks and are an intriguing alternative for the future. In order to develop the technology, there is a need for fundamental research into all the aspects of energy conversion in such devices and one relevant topic is that of charge transport.

This thesis is based on work done in the Biomolecular and Organic Electronics group at the Department of Physics, Chemistry and Biology, Linköping University, under the supervision of Professor Olle Inganäs.

Not only has Olle managed to gainfully supervise this work in his own lab, he has also arranged for extended visits to other labs and an acknowledgement of the following people and their research groups is thus in order:

Professor Henrik Stubb and Professor Ronald Österbacka at the Department of Physics, Åbo Akademi University, who in many ways rendered this work possible.

Professor Gytis Juska at the Department of Solid State Electronics, Vilnius University, who is an inexhaustible source of information on charge extraction.

Professor Tomoji Kawai and Professor Takuya Matsumoto at Kawai lab, Osaka University, who introduced me to force microscopy based electrical measurements.

Obviously, all the members of these research groups have been valuable, some more than others. It would, however, be a Sisyphean task to list everyone without

forgetting someone important. Anyone that feels that they may have contributed has my thanks.

Linköping, September 2007
Mattias Andersson

Contents

CHAPTER 1

Humidity Sensors and Bolometers (Introduction)

If all that the world needed was a bunch of humidity sensors and bolometers, then organic electronics would most definitely be a viable alternative. Unfortunately the need for transistor logic far outweighs the need for humidity sensors and solar cells are, in a general sense, a lot more useful than bolometers, so there are some issues to iron out before organics will replace silicon as the material of choice for our semiconductor needs.

It does not end with water and electromagnetic radiation; organic semiconductors, or at least many of the pertinent device geometries used, are sensitive to, take or leave a few items, everything. This makes characterization a bit of a chore, and seemingly trivial measurements can require some consideration to realize properly, especially since many materials have a limited processability and availability.

There has been a lot of work done on charge transport in organic solids in the literature but much of it does not properly address the general sensory nature of the materials or the dynamic aspects associated with charge transport in this class of materials. Theories and explanations for observed phenomena are abundant and frequently have a very narrow field of application, where different theories are used for different device geometries. Recently there has been some movement towards a unified theoretical picture, and while many of the theories that have been used to explain specific device phenomena may still hold some merit, there is not yet sufficient experimental poise in the community to properly assign partial contributions of various kinds to observed phenomena in any great detail. As such, it is useful to take a step back and try to conciliate available data in a broad sense using only a minimum of theoretical minutiae. The introduction to charge transport in organic materials given here aims to do just that; it is a very fundamental description and there are many details and some theory that are purposefully omitted in order to emphasize the basic concept and fundamental implications of hopping transport.

Basic sample geometries and measurement techniques are presented with the intention of emphasizing the experimental difficulties imposed by organic materials, both in terms of acquiring and evaluating data.

Everything is first and foremost done with solar cells in mind and that is reflected in the way certain aspects are presented. Transistors, for instance, are always primarily considered as a material characterization tool, and as such, some of the discussion on that topic is seemingly irrelevant when it comes to state of the art organic transistors. Only a small number of materials are explicitly included here, but measurements have been done on a lot of materials with very varying properties and many conclusions are based on accumulated experience.

CHAPTER 2

Electronic Transport Theory

2.1 Electronic Structure

2.1.1 Density of States

A materials density of states is a measure of the number of allowed energy levels as a function of energy. An allowed energy level can be occupied or unoccupied. Without going into any detail it can be mentioned that electrons are considered indistinguishable, are labeled as Fermions, obey the Pauli exclusion principle, and that two electrons can occupy each energy level. Beginning with the lowest energy level and going up, all the electrons in a system are then associated with an energy level. The energy up to which all the levels are filled is called the Fermi level. At temperatures above $0K$, thermal excitation occurs and there will be vacancies below and occupation above the Fermi level. The energy levels are grouped together in energy bands where the separation between the energy levels is small, and the bands are separated by a much larger energy difference. If the Fermi level is positioned in the middle of an energy band, the material is a conductor, if the Fermi level is positioned between bands and the separation is big, the material is an insulator, and if the Fermi level is positioned between bands but the separation is small, the material is a semiconductor. The requirement for conduction is that there are vacant states available within a partially filled band for an electron to move to. It is thus perfectly possible for every material, including insulators, to conduct electronic current but insulators need to have the number of electrons manipulated so that there is a partially filled band available. Almost all the properties of a material that is of interest here are determined by the electronic structure around the Fermi level. The highest (at $0K$) fully occupied band is commonly referred to as the valence band, the lowest unoccupied band is referred to as the conduction band and the separation between the valence band

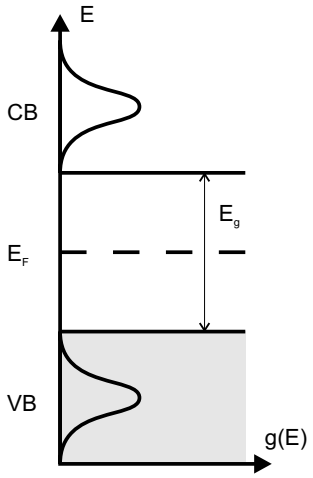

Figure 2.1. Schematic band structure around the band gap.

and the conduction band as the band gap (Figure 2.1). For a semiconductor it is usually enough with thermal excitation or the addition of trace amounts of impurities to get electrons from the valence band and into the conduction band. An additional worthwhile definition is that of the work function, which is measured from the vacuum level to the Fermi level.

2.1.2 Conductivity

The number of electrons in the conduction band and holes in the valence band and their their respective mobility, all of which is determined by the electronic structure, determines the electronic conductivity of a material through Equation 2.1, with q beeing the elementary charge, μ_n, μ_p and n, p, the mobility and concentration of electrons and holes respectively. Assuming that there is an easy way to get a substantial amount of carriers into the conduction band, the important quantity to consider is the mobility. This is indeed the case for many applications and is especially true here. Both FETs and solar cells operate with a limited amount of extra charge. FETs are operated by modulating the amount of charge in the appropriate band, and the resulting current modulation is thus directly proportional to the mobility. In solar cells where carriers are generated by the incoming photons and disappear through recombination the amount of charge that is possible to extract is also in many ways connected to mobility.

$$\sigma = q(n\mu_n + p\mu_p) \tag{2.1}$$

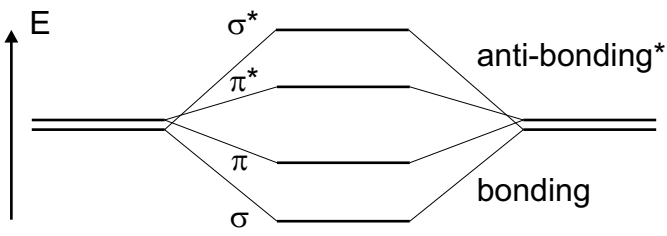

Figure 2.2. Energy level splitting upon bond formation.

2.1.3 Polymeric Semiconductors

When two atoms are brought together and they are capable to form a covalent bond they will share some of their valence electrons with each other. How the electrons are shared determines the nature of the bond. The electrons of an atom are spatially distributed over a set of orbitals defined by probability. Some of the electrons have spherical iso-probability while others have much more elaborate orbitals. The first few have names derived from their spectroscopic properties and the first two are labeled s for sharp of which there is one for each shell, and p for principal of which there are three for each shell, with shell in some sense a measure of the distance from the core. S-orbitals are spherical and p-orbitals resemble the figure 8. When atoms are brought together their respective orbitals interact with each other to form a new set of molecular orbitals, and the shape and properties of the product is to a large extent determined by the participating atomary orbitals. Energy wise, the atomic valence orbitals of the constituent atoms are split up into bonding and anti-bonding molecular orbitals. Depending on the way electrons are shared, different types of bonds are formed. A pair of atomic orbitals that points straight at each other leads to a bond where the participating electrons are strongly localized between the bonding atoms in a σ-bond. Orbitals that are parallel to each other have considerably less localized electrons, labeled π-electrons, and form a π-bond, which together with a σ-bond makes a double bond (or a triple bond if an additional π-bond is added). The splitting of the energy levels upon bond formation is shown schematically in Figure 2.2, and σ and π orbitals are visualized in Figure 2.3.

The carbon atoms of the conjugated polymer backbone bind to three other atoms and thus form three σ-bonds and one π-bond. Figure 2.3 shows the valence orbitals of one of the backbone carbons. In the lower part of the picture the orbitals have been separated for clarity. This orbital configuration is commonly referred to as sp^2 hybridization, which means that one s-orbital and two p-orbitals have been hybridized to give the three σ-bonding orbitals. The remaining p-orbital is responsible for the π bond and is referred to as a π-orbital. Hybridization theory is simply a useful tool to get an idea of how a molecule will likely look. In reality the actual molecular orbitals might look quite different but the predicted presence of π-orbitals and their properties is accurate. The weak bonding character of the π-orbitals also means that the associated anti-bonding orbitals have only a weak

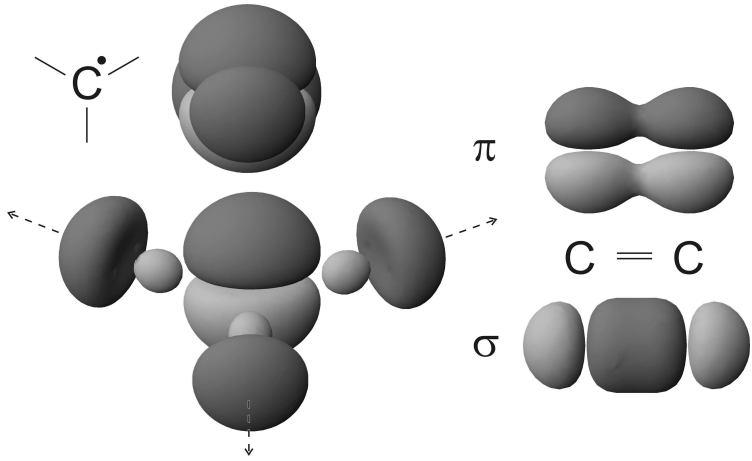

Figure 2.3. Iso-probability surfaces of various orbitals.

anti-bonding character. Consequently, the bonding π-orbitals define the HOMO and the anti-bonding π-orbitals define the LUMO of a conjugated polymer, and the energy gap between the HOMO and the LUMO is much smaller than would be the case if only σ-bonds were present.

2.1.4 Mobility

The density of states in the valence and conduction bands can be directly correlated to the chemical structure of the material. All atoms contribute to a potential landscape and if the system is highly ordered, the spread in energy is small and the density of states large (Figure 2.4a). If there is positional disorder in the system the energetic spread will increase and density of states decrease (Figure 2.4b). Impurities also influence the DOS but tend to add states at some specific energy without greatly affecting the main DOS of the material (Figure 2.4c). When the site density is high, such as in crystals, the localization radius of an electron is large, and if sufficiently large it is said to be delocalized and is no longer associated with a particular atom. When the site density is low, the localization radius is smaller and the electrons become localized. The less localized the electrons, the higher the mobility and the transition from localized to delocalized states is labeled as the "mobility edge" (Figure 2.5) [1] [2] and marks a transition in transport mechanism from the hopping between sites necessary for localized electrons to the ballistic transport of delocalized electrons. Almost all polymers, and certainly all the amorphous ones, only have localized states and are thus subject to hopping transport. A perfect conjugated polymer chain can at first glance seem to be a one dimensional crystal, this is not true, however, as Peirels [21] [22] showed that such a system needs to dimerize to become stable. This dimerization causes a bigger perturbation to the potential than would only the atom cores, thus caus-

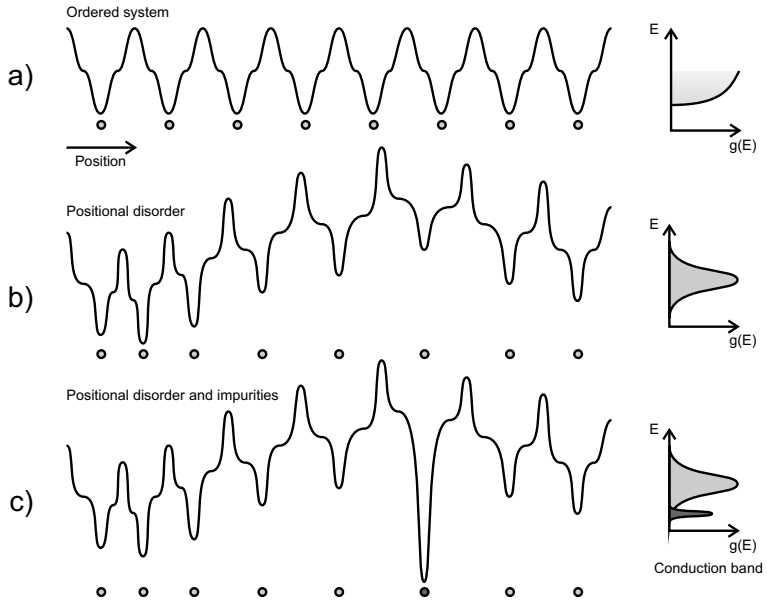

Figure 2.4. DOS and structure correlation.

ing localization also in a perfect conjugated polymer chain. There is a difference between the potential fluctuations caused by externally induced disorder and that caused by dimerization; the former is imposed on the system due to external influences, the latter is strongly associated with the electrons and can move. An added electron to a conjugated polymer chain causes a distortion of the dimerization and generates its own potential well, which then can travel along with the electron. This is a quasi particle labeled a polaron (The name comes from polar crystals, where the phenomenon was first encountered.). [9] [10] There are other quasi particles that are related to the polaron such as bipolarons. In the highly disordered systems discussed here, polarons are of small consequence to the electronic transport properties at room temperature but may be important at lower temperatures.

2.1.5 Traps

Few concepts are so freely used with as many meanings, as traps within the field of organic electronics. When transport is ballistic the concept is simple; a trapped carrier is just that. It is trapped and does not, at that particular moment, move, and does thus not contribute to the conduction. As the focus has changed towards more disordered materials with hopping transport the term has stayed in use but with a more ambiguous meaning. All the carriers are in essence trapped in a highly disordered material and while there may certainly be trapping by impurities, it is not necessarily possible to distinguish thus trapped carriers from those in low

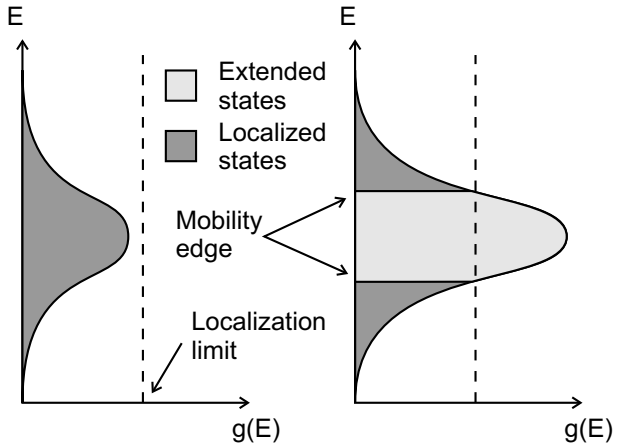

Figure 2.5. Localized and extended states.

energy states in the main density of states. If there is an increased site density at some fairly narrow energy interval that is possible to link to an impurity, and that have a significant impact on the transport properties, it can still be useful to talk about traps in the traditional sense but if there is no obvious and clearly defined trap level it is best to consider the impurity states as simply a part of the density of states without disambiguity.

2.2 Gaussian Disorder Model, GDM

A localized electron can hop to a different site either by thermal activation where the thermal energy excites the carrier so that it can overcome the potential barrier between the sites, or by tunneling through the barrier. Activated hopping is by far the most dominant mechanism at room temperature and the most useful transport model is thus based on this concept. Such a process is very easily simulated with the Monte Carlo method, which is the basis of the the Gaussian Disorder Model, GDM [4]. The GDM assumes a Gaussian energy distribution of the carrier transport sites, and a Miller-Abrahams type [16] jump rate between sites. Equation 2.2 is a Gaussian of width σ, used to approximate the DOS of either the valence or the conduction band and E denotes energy. Equation 2.3 is the product of a prefactor ν_0, an electronic wave function overlap factor where γ is the inverse of the decay length of the localized wave functions and ΔR_{ij} is the distance between sites i and j with energy ϵ_i and ϵ_j respectively, and a Boltzmann factor for jumps upward in energy. Carriers in such a DOS will themselves have a Gaussian distribution of the same width as the DOS, and which at low carrier concentrations is centered at $-\sigma^2/kT$ with respect to the DOS (Figure 2.6). In reality things are more complicated, and a simple Gaussian might be too rough an approximation for many systems and the hopping might be of a different kind, but

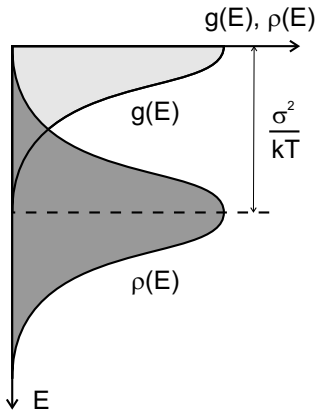

Figure 2.6. DOS ($g(E)$) and occupied DOS ($\rho(E)$).

there has been a lot of work, both experimental and theoretical, done within the model and it is thus useful as a starting point for phenomenological discussions and predictions. Two of these predictions; the temperature dependence and carrier concentration dependence of the mobility will be discussed in more detail here. A useful definition is the effective disorder parameter, $\hat{\sigma} = \sigma/kT$, which is often the relevant parameter when describing a system.

$$g(E) = \frac{1}{\sqrt{2\pi}\sigma} exp\left(-\frac{E^2}{2\sigma^2}\right) \tag{2.2}$$

$$\nu_{ij} = \nu_0 exp(-2\gamma\Delta R_{ij}) \begin{cases} exp\left(-\frac{\epsilon_i - \epsilon_j}{kT}\right); & \epsilon_j > \epsilon_i \\ 1; & \epsilon_j < \epsilon_i \end{cases} \tag{2.3}$$

2.2.1 Mobility and Carrier Concentration

When the carrier concentration increases above a certain level, the offset between the center of the DOS and the average carrier energy will decrease. Again using the transport energy concept, it is reasonable to assume that as this offset decreases, so will the required activation energy. At the same time, the number of available sites to jump to will increase for the average carrier, since the DOS is the largest at the center. There is, of course, an exception for very high carrier concentrations where the neighboring sites of a carrier starts to have a high occupation probability and the number of available sites thus decreases. Since the hopping rate, and thus mobility, is dependent on the number of accessible sites for an average carrier, the mobility will increase with increasing carrier concentration. The mobility concentration dependence is in turn strongly dependent on the amount of disorder in the system or, concomitantly, the width of the DOS. More disorder gives stronger concentration dependence [20] [5]. The mobility enhancement as a function of carrier concentration for some reasonable DOS widths at

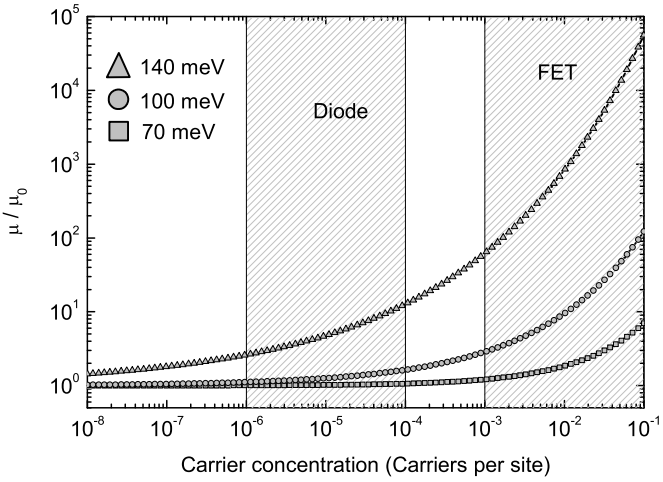

Figure 2.7. Mobility concentration dependence according to Equation 2.4 for different DOS widths at room temperature.

room temperature is shown in Figure 2.7, and is based on a parameterization of numerical simulations (Equation 2.4).

$$\mu(c) = \mu(0)exp[u(2c)^v] \tag{2.4}$$

with

$$u = \frac{1}{2}\hat{\sigma}^2 + ln2 \tag{2.5}$$

and

$$v = 2\frac{ln(\hat{\sigma}^2 + ln4) - ln(ln4)}{\hat{\sigma}^2} \tag{2.6}$$

2.2.2 Mobility and Temperature

If the presence of a mobility edge is assumed, and transport is considered as of a multiple trapping and release kind, where the transport energy is that of the mobility edge, it is possible to conclude that the activation energy is proportional to the offset of the occupied DOS. In reality there is likely no mobility edge, but the predicted activation energy and the resulting non-Arrhenius type temperature dependence has been observed experimentally. As a first order approximation, the temperature dependence is described by Equation 2.7 and the activation energy as Equation 2.8. In general, the temperature dependence of the mobility is very strong around room temperature. At elevated temperatures, close to the glass

transition temperature or melting point of a material it obviously deviates from the predictions but this is usually also the case at lower temperatures where it usually is much weaker than indicated by Equation 2.7. The main reason for this is likely the carrier concentration dependent mobility. As temperature decreases, the effective disorder parameter increases, leading to an increase in mobility enhancement with decreasing temperature. It should be pointed out that some efforts have been made in the literature to explain the low temperature behavior with a transition from transport in the main DOS to transport within trap levels of the DOS [3], with a transition from non-dispersive to dispersive transport [18], a change from the Miller-Abrahams type hopping to some other means of electron transport such as non-adiabatic small polaron hopping or tunneling [13], or a transition from small to large polaron hopping. [29] Although none of these theories are necessarily wrong, they are all unable to consistently explain experimental data on their own, but they may well contribute to the real behavior. Examples of temperature dependence that takes carrier concentration into account by way of Equation 2.4 is shown in Figure 2.8. As the temperature decreases the parameterization in Equation 2.4 fails and the physics of the transport may change. Because of this the temperature range in which the model is appropriate is limited. Different parameterizations may be used for different disorder and temperature ranges but the physical limitations are still there.

$$\mu(T) = \mu(0) exp\left(-\frac{E_a}{kT}\right) \tag{2.7}$$

$$E_a = \frac{4}{9}\frac{\sigma^2}{kT} = \frac{4}{9}\sigma\hat{\sigma} \tag{2.8}$$

2.3 Amorphous Polymers vs. Inorganic Crystals

A very large portion of all electronics is based on crystalline silicon, and since much of the higher order theory is recycled for amorphous polymers it is worthwhile to point out some of the differences between the ballistic transport of electrons in crystals and the hopping transport in amorphous materials in more detail.

2.3.1 Band Edges

Crystalline materials have very well defined bands, and an unambiguous definition of ionization potential and electron affinity is possible; from the top of the valence band, or HOMO, and the bottom of the conduction band, or LUMO, respectively. Disordered materials lack well defined band edges and their positions are difficult to measure. HOMO and LUMO is therefore used rather arbitrarily to define energy levels reasonably close to the true values but where the DOS is significant. More often than not, this means that there will be a discrepancy between, for instance, the onset of optical absorption and the HOMO-LUMO difference (Figure 2.9).

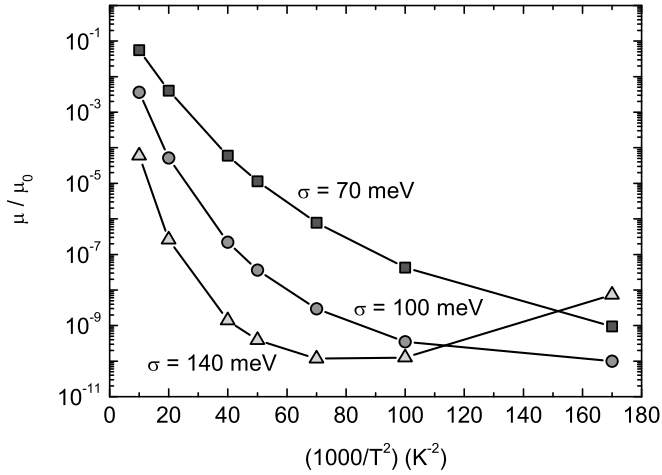

Figure 2.8. Temperature dependence of a carrier concentration dependent mobility for different σ. Carrier concentration is 10^{-4} carriers per site.

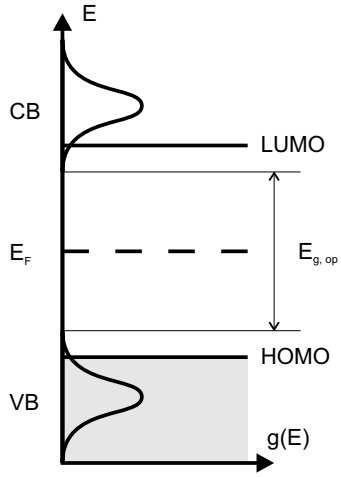

Figure 2.9. Habitual careless HOMO-LUMO use.

2.3.2 Temperature

The mobility decreases strongly with decreasing temperature for activated transport of the kind exhibited by most polymers at and around room temperature. Ballistic transport does not require any activation and the mobility is instead limited by scattering events. Scattering can be due to impurities or phonons. Phonon scattering will decrease with decreasing temperature and the mobility will thus increase. The temperature dependence of mobility in polymeric devices is the opposite to that of their crystalline counterparts.

2.3.3 Anisotropy

The anisotropy in polymeric materials can potentially be much larger than in covalent crystals with symmetric unit cells. In very amorphous polymer systems there is hardly any anisotropy but polymeric crystals can have a considerable anisotropy.

2.3.4 Carrier Energy

Ballistic transport occurs because there are plenty of available states over which a carrier can be delocalized and there is no real difference for a carrier with a small amount of excess energy. For hopping transport there is always an increase in accessible states when excess energy is added to a carrier. The result is an energy dependent mobility. [23] This takes many forms and can, for instance, be seen experimentally as an electric field dependent mobility. When charges are introduced in the system at an elevated energy there will also be a time dependence in the mobility as the excess energy is dissipated. [12]

2.3.5 Doping

When dopants in the form of impurities are introduced into a crystal they act as scattering centers and the mobility is decreased. When an electron is added or removed from a polymer chain the rest of the pi electrons gets a bit more delocalized in order to help compensate the change in charge. This can straighten an otherwise winding polymer chain and decrease the energetic distribution of sites with a resulting increase in mobility.

2.4 Current Injection

Direct electrical measurements on materials such as conjugated polymers require appropriate contacts. In some cases, such as in transistors, good ohmic contacts suitable for injection is desired, while in other cases, such as with charge extraction experiments, blocking contacts are necessary. For commercial applications where the device properties are critical, a lot of effort might be required to get sufficiently god contacts. When the purpose of different devices is solely to facilitate measurements there is less need for a very rigorous treatment but it is still

worthwhile, and necessary, to consider the problem on a phenomenological level. Many polymers and all heterogeneous blend systems are ambipolar and can thus transport both electrons and holes to a fairly similar extent. This means that most contacts are more or less injecting for one carrier type, and more or less blocking for the other type. In fact, most simple contacts fall into the category "poorly injecting", which is actually quite useful since it can be used as both injecting and blocking depending on bias.

2.4.1 Metal-Semiconductor Contacts

The simplest and most common type of contact, where a metal is brought into contact with a semiconductor, will have properties based upon the work function of the metal (Φ_M) and the electronic structure of the semiconductor (HOMO, LUMO, and semiconductor work function Φ_S). Charges will be transferred across the junction so that the Fermi levels (E_{FM}, E_{FS}) align. If majority carriers are injected into the semiconductor it is an ohmic contact, and if they are extracted from the semiconductor it is blocking. [15] The charge transfer across the junction gives rise to band bending in the semiconductor and a contact potential ($\Delta\Phi$). The width of the region required to accommodate the contact potential (W) is dependent on the magnitude of the potential and the carrier concentration in the semiconductor such that a large contact potential and a low carrier concentration in the semiconductor give a large W. As long as the work function of the metal is lower than the ionization potential (E_I) and higher than the electron affinity (E_{EA}) of the semiconductor there will also be an injection barrier (Ψ) associated with the contact. Figure 2.10 shows a hole injecting and a (hole) blocking contact to a moderately p-type semiconductor.

2.4.2 Transistor Contacts

To make proper ohmic source and drain contacts to a transistor would require different metals for p- and n-type devices. Polymer HOMO levels are frequently around $6eV$ and their LUMO levels around $4eV$, which means that very few metals are able to form really good contacts. Taking into account that low work function materials are easily oxidized in air and that the work function of high work function materials usually is substantially reduced by atmospheric contaminants there are precious few simple choices. A very common electrode material for p-type devices is gold. Reasonably clean, as in cleaned gold in ultra high vacuum, has a work function of about $5.4eV$ (CRC handbook), but this is reduced to somewhere around $4.3eV$ when exposed to air, a value that in theory would not make for a good hole injecting contact to a polymer with a $6eV$ HOMO level. It turns out, however, that not only does gold work fine for p-type devices; it also works well for n-type materials and devices. The reason for this is that an applied gate bias induces carriers into the channel near the contacts and this moves the Fermi level closer to either the HOMO or the LUMO according to the applied bias. Due to the high carrier concentration under bias, the contact potential zone is very narrow and tunneling can easily occur between the metal and the appropriate semiconductor

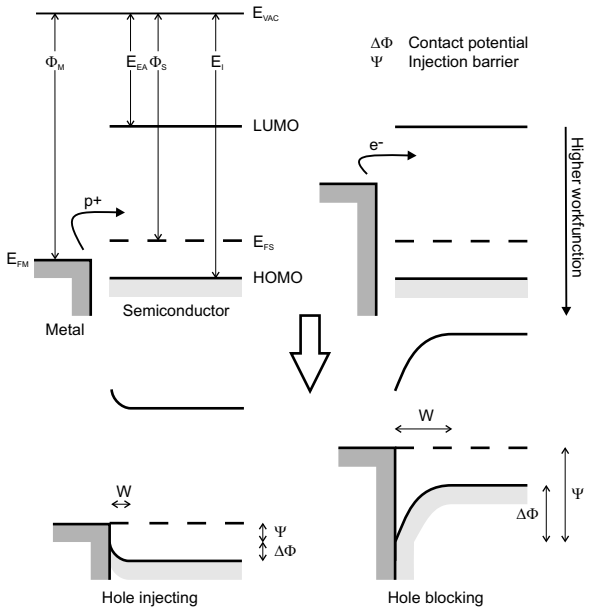

Figure 2.10. Hole injecting and hole blocking (electron injecting) metal-semiconductor contacts.

band.

A reasonable approximation to a gold-polymer contact is shown in Figure 2.11. Without applied gate bias there are high barriers for injection of either type of carrier and as bias is applied, injection through tunneling becomes possible.

2.4.3 Diode Contacts

In a diode configuration where there is no gate modulation of the carrier concentration the situation is that of an unbiased transistor and the demands on the contact materials are thus higher. For device applications, such as light emitting diodes or solar cells, it is usually desirable to have one electron injecting and one hole injecting contact. Such a device is rectifying. Under forward bias both electrodes are injecting for their respective type of carrier and under reverse bias both are blocking. Experimental techniques, such as time of flight and charge extraction by linearly increasing voltage, require blocking contacts and it is thus possible to use standard devices under reverse bias. There are drawbacks with this though, and this is discussed in the appropriate sections on the measurements. Suffice to say there are reasons to want contacts that are blocking for both bias directions. This is fairly straightforward in unipolar devices where either two high work function or two low work function materials can be used for the contacts, but is more difficult for ambipolar materials, where instead the electrode work functions have to be chosen so that they are close to the middle of the semiconductor band gap. The polymer layer in organic devices is usually quite thin, and the injecting fields

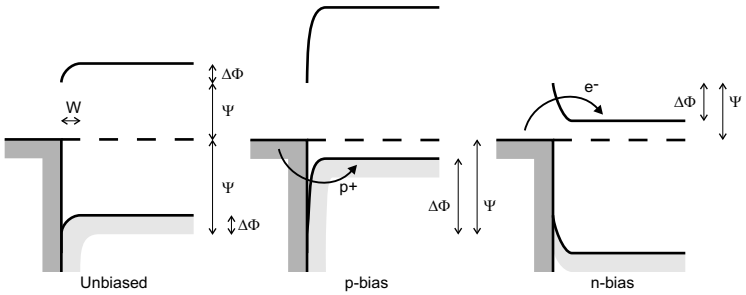

Figure 2.11. Gold-polymer contact under various bias.

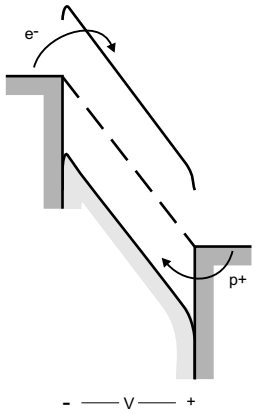

Figure 2.12. Enhanced injection at high bias.

are thus high. Totally blocking contacts are therefore not able to stand very high voltages before the injection barriers are overcome (Figure 2.12).

CHAPTER 3

Field Effect Transistors

3.1 General Principles

The field effect transistor, or FET as it is more commonly known and henceforth referred to, is the most common of today's transistor types and is the fundamental building block in all CMOS (Complementary Metal-Oxide Semiconductor) logic. It utilizes an electric field to manipulate the charge carrier concentration at the interface between an active material and an insulator and thereby modulating the conductivity along the interface. The electrode used to generate the modulating field is commonly referred to as "gate". Two electrodes are used to define a "channel" along the interface and these are commonly referred to as "source" and "drain" which for the most common type of transistor, n-type enhancement mode, refers to current flowing in the direction drain to source in the on-state. In a standard CMOS transistor, the source and drain electrodes consists of moderately doped silicon (n or p), whereas the channel has weak doping of opposite type. The gate is a metal conductor. There is no fundamental need for asymmetry in a FET and the source / drain electrodes can be identical but in practical applications there is frequently a small difference in order to optimise the normally unidirectional current flow. Figure 3.3 in Section 3.2 shows the semi-organic counterpart to a Si-FET.

3.1.1 Terminology

Threshold Voltage

In order for current to start flowing in an enhancement mode device, it is necessary to overcome the weak channel doping (which is of opposite sign to that of the desired cannel) before current will start to flow. This means that a certain gate

potential has to be applied before modulation takes place and this is termed the "threshold voltage" of the device.

Enhancement and Depletion Mode

In enhancement devices, which by far are the most common type, the gate potential is used to create a conducting channel, whereas in depletion devices the gate potential is used to prevent conduction in the channel (by depleting the carriers).

Current Saturation

In order for a current to flow through the device it is obvious that a potential difference between drain and source is required. This potential will affect the channel since it is the potential difference between the gate and the channel that modulates the number of channel carriers. The potential difference between source and drain will give a gradient in channel carrier concentration. When the potential of one of the electrodes is sufficiently close (gate potential minus threshold voltage) to that of the gate, so that there will no longer be an enhancement of the desired carrier type in the channel near the electrode, "pinch off" will occur. During pinch off the source / drain current will be practically independent of a further increase in potential and the device is said to operate in "saturation".

3.1.2 Transistor Measurements

Transfer Characteristics

There are many ways to extract information from a transistor and one common way is to use transfer characteristics, where a constant source / drain potential is applied and the gate potential is swept between some suitable values. From this type of measurement it is possible to extract charge carrier mobility in the channel and threshold voltage, among other things. If the device is biased in the saturated regime, the mobility is given by the slope of the square root of the source / drain current through Equation 3.1, where W is the channel width, L the channel length, C_i the insulator capacitance per unit area, I_S the source / drain current, and V_G the gate voltage. Ideally, the square root of the source / drain current is a straight line and its intersect with zero current gives the threshold voltage. A SPICE simulation of a transfer characteristic of an inorganic transistor is shown in Figure 3.1.

$$\mu = \left(\frac{\partial \sqrt{I_S}}{\partial V_G} \right)^2 \frac{2L}{WC_i} \tag{3.1}$$

Output Characteristics

To prove proper transistor operation it is common to use the output characteristics, where the channel current is plotted as a function of source / drain potential

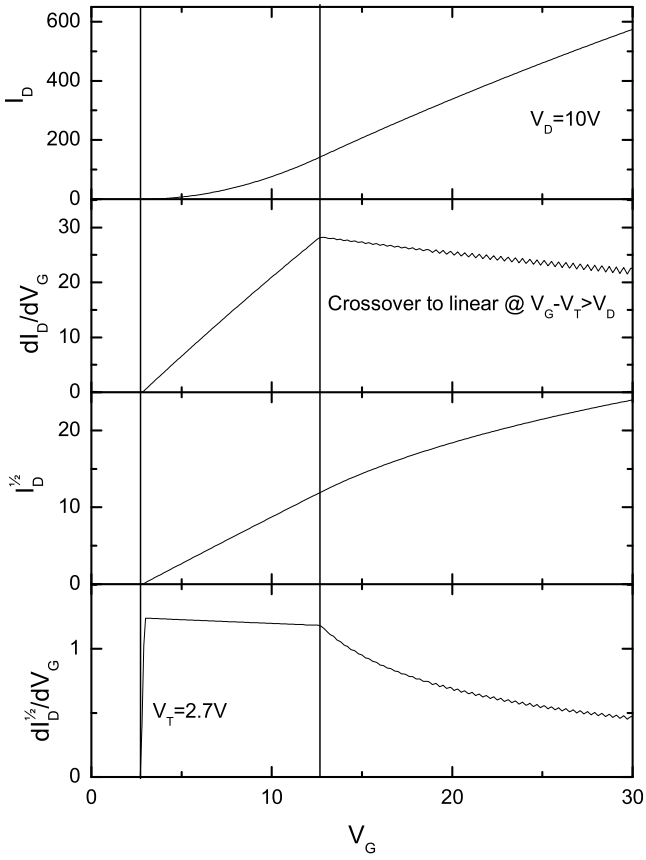

Figure 3.1. SPICE simulated transfer characteristics.

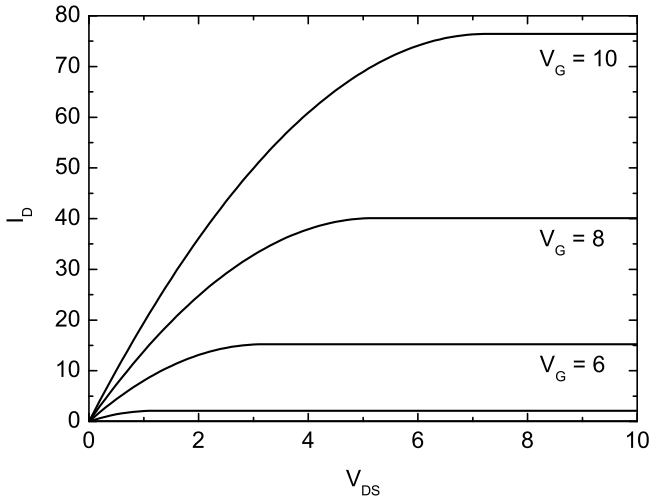

Figure 3.2. SPICE simulated output characteristics.

for different gate potentials. As far as a simple visual inspection goes, it contains more information about the behaviour of the device than does a transfer characteristic but to obtain mobility values from the data it is necessary to have the threshold voltage of the device, and this is generally obtained from the transfer characteristics. A SPICE simulation of an output characteristic is shown in Figure 3.2.

3.2 Organic Field Effect Transistors

The principle of operation of an organic FET (OFET) is the same as in the inorganic case and there are many similarities. This has led to a very far-reaching adaptation of nomenclature and characterization theory from silicon devices. There are, however, many differences and while the end results may look similar, the underlying physics is sometimes very different. The term OFET, or any of the numerous analogue terms used, can mean many things but is commonly used for devices where the active part of the transistor, the channel, is an organic material. Any other parts of the transistor can still be inorganic. When the main purpose of the OFET is as a characterization tool for organic materials it is often convenient to use silicon-based substrates with lithographically patterned electrodes that are easy to mass-produce. All-organic devices are certainly possible but the added effort required producing them means that they are only used when specific reasons dictate or when the purpose is to make devices rather than material characteriza-

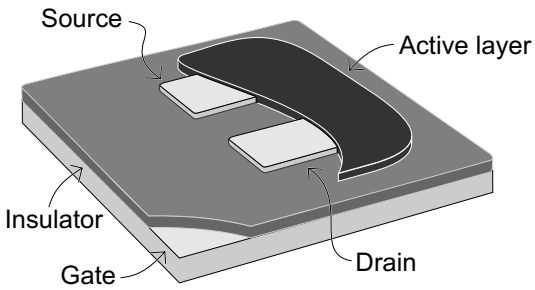

Figure 3.3. Typical OFET.

tion. A typical OFET for material characterization is shown in Figure 3.3.

As polymers are permeable to, among many other things, oxygen and water and these acts as electron traps and p-dopants in polymers, most OFETs operated in air are of p-type character. This also indicates a difference to inorganic devices where n-type devices are made of p-type materials and vice versa. Organic transistors are mostly p-type devices made of p-type material. Coupled with the fact that the doping of organic materials frequently is unintentional and in any case much less defined than for inorganics this gives devices that can conceivably be somewhere between depletion and enhancement mode. Another noticeable difference lies in the mobility; not only is it much lower than for crystalline silicon, it is also based on a completely different kind of electronic transport and the dependence on parameters such as temperature and carrier concentration is thus also completely different.

3.2.1 Mobility Measurements

FETs almost always operate in a range where carrier concentration has a profound impact on mobility. The carrier concentration is determined by the gate voltage, but is usually not known. To put a number on it requires some rather arbitrary assumptions regarding site density and channel height. During a transfer measurement it is thus reasonable to expect a varying mobility but it is not, as per Section 3.2.2, very easy to predict. Any mobility values extracted from such a measurement will thus be greatly influenced by the measurement conditions and data evaluation. Although there is little merit to the actual mobility numbers obtained it is still possible to determine if the mobility is high or low, and as long as the appropriate precautions are taken it is perfectly possible to discern various trends and dependencies from FET measurements. Most of the included papers, especially Paper II, elaborates on the validity and usefulness of FET measurements as a tool for material characterization.

3.2.2 Mobility Measurement Issues in Polymer Devices

Low Mobility

An unusually low mobility in an organic material presents a unique problem. The transit time of a carrier through the channel can be much longer than the acquisition time for a data point in the measurement. Since the channel formation most certainly involves charge injection from the electrodes this means that until the channel is completed there will be a noticeable difference between source and drain currents. The current at the injecting electrode behaves normally but there is a delay before the current rises at the extracting electrode. When the channel formation is complete, the current at the extracting electrode will rise quickly to the level of the injection current (Figure 3.4). If threshold voltage and mobility is calculated based on the current from the extracting electrode, there will be an overestimate of both the mobility and the threshold voltage. Considering the very special nature of organic semiconductors where the threshold voltage often is very stress sensitive, and that the currents are already low in a low mobility material, it is not always straightforward to remedy the problem simply by increasing the measurement time. Simply using only the current at the injecting electrode is often sufficient. For channel lengths of around $10\mu m$ and a total measurement time of a few seconds this becomes an issue for mobilities of $10^{-5}cm^2V^{-1}s^{-1}$ and below.

Another effect is that there will be a visible extraction current after the gate potential is reduced below the threshold voltage to the off state of the transistor. This can also lead to a misestimation of the threshold voltage but again it is simply a matter of using the current measured at the other electrode. A crossover of the outgoing and ingoing current sweeps in the transfer characteristic is usually a good indication of this problem.

Contact Resistance

When standardized test substrates, typically with gold electrodes, are used, there is always a risk of poor injection and high contact resistance. If the studied material has a high mobility, the channel resistance becomes comparable to the contact resistance, which will thus influence the measurement. The contact resistance can vary several orders of magnitude between different materials and conditions and it can be difficult to determine if an observed behaviour is due to contact resistance or something else. Both the source and the drain have contact resistances associated with them and the influence on transistor behaviour is slightly different. The insert of Figure 3.5 shows a transistor with explicit contact resistances. It has its source connected to reference ground and its drain connected to the appropriate drive potential. If the source and drain resistance are equal there will be an equally big potential drop over both contacts. The drain resistance merely reduces the source-drain potential of the channel proportional to the circuit current, while the source resistance, on the other hand, reduces both the source-drain potential of the channel and the effective threshold voltage. How much the effective potentials are reduced, as a function of contact resistance to the transconductance of the

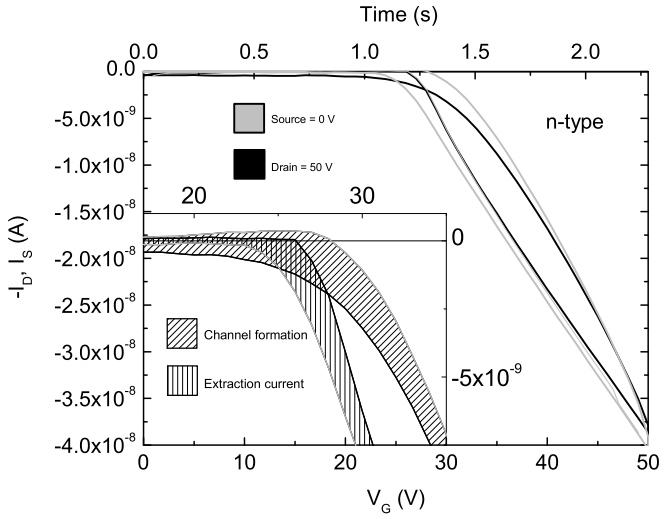

Figure 3.4. Low mobility channel dynamics.

transistor is shown in Figure 3.5. As long as the contact resistance - transconductance product is below 0.01 there is hardly any influence and the difference is still small at 0.1. In terms of real devices, this roughly translates to only being a real problem for mobilities around or above $10^{-3}cm^2V^{-1}s^{-1}$. Disregarding any other effects, it is possible to see a large drain resistance as a clearly sub quadratic transfer characteristic at high gate potentials. There will also be a larger than expected dependence on device geometry.

Channel Length

Carriers are injected into the channel at the Fermi level and then relax toward energetic equilibrium with time. If the channel length is short enough so that the carrier transit time is comparable to the relaxation time there will be a strong channel length dependence of the mobility. This is because of the increased mobility associated with the added energy of the injected carriers compared to the equilibrium carriers. As the channel length, and concomitantly the transit time, increases the device characteristics will approach equilibrium values. For this reason it is useful to compare the mobility for different channel lengths to determine if it really is equilibrium characteristics that are probed.

Bias Stress and Hysteresis

One of the most defining characteristics of OFET is their predisposition for bias stress. The nature of bias stress is handled more elaborately in Paper I and in

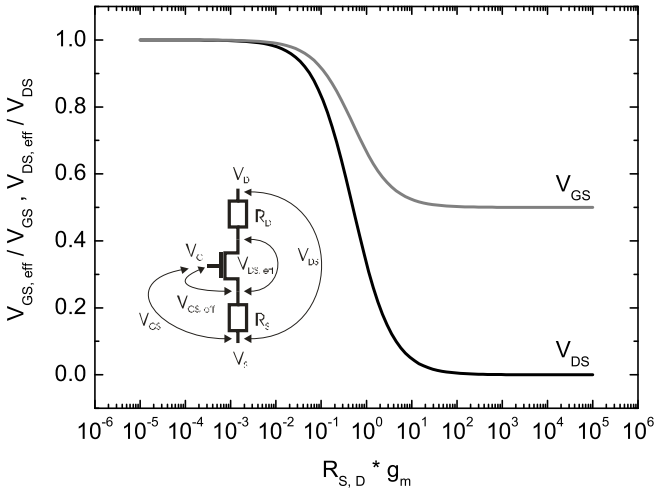

Figure 3.5. Impact of contact resistance on the effective transitor bias.

Section 7.1, but as a first order approximation the effect is well described by a time and gate voltage dependent threshold voltage. This means that the channel current of a device is time dependent and that the time dependence is in some way proportional to the bias. Similar effects are seen in many other disordered materials such as amorphous silicon, but they are slightly different in nature and, at least in part, do not have the same origin. Like contact resistance, bias stress can lead to a sub quadratic current in the transfer characteristics for off-to-on sweeps. For an on-to-off sweep the current is instead super quadratic. The effect is severe and appears as hysteresis in measurements. Given enough time possibly all devices will completely turn themselves off due to that the threshold voltage has shifted all the way to the applied gate potential. All materials are different though, and the timescale of the bias stress varies with many orders of magnitude between different materials. There is no simple way of quantifying bias stress. Perhaps the scientifically best way, without very elaborate measurements involving local potential in the channel [28], is as the difference in threshold voltage for a set biasing procedure. Other schemes, such as various current ratios are also possible. Although none of the methods is very accurate, it is still possible to establish various dependencies from these simple estimates.

3.2.3 Threshold Voltage in Polymer Devices

The threshold voltage for simple p-type OFET has traditionally been expected to be zero or positive based on the theory for inorganic devices. In reality, there is

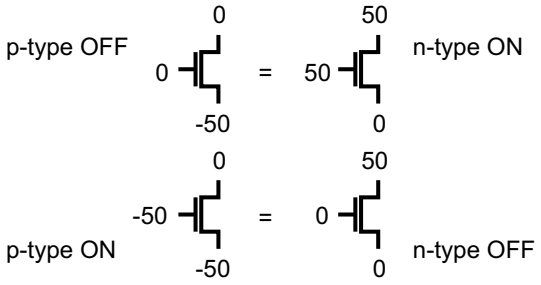

Figure 3.6. Bias universality.

frequently a very large negative threshold voltage. As is obvious from the discussion on bias stress, the value is also unstable. To know if the threshold voltage has shifted requires a measurement, and if only simple i/v measurements are available, that measurement will likely stress the device so that the threshold voltage shifts. Measurements of threshold voltage in many materials are therefore very difficult to get reproducible with any accuracy, given that recovery can sometimes be extremely slow, on the order of hours or days. When transistors are only used as a characterization tool, there is no real need to have an accurate threshold voltage unless evaluation is done from output characteristics, and given the instability of the threshold voltage this is not advisable.

Ambipolarity

Although most polymeric materials behave like p-type on silicon oxide in air, most of them are actually ambipolar. A few materials, more if the gate insulator is substituted for a hydrophobic alternative and even more if the measurements are done in vacuum, show ambipolar qualities and this influences mobility evaluation. Obviously, the following discussion is valid also for two-phase systems that are deliberately ambipolar such as polymer / fullerene blends. Figure 3.6 shows that from a biasing point of view, the off-state of a p-type device is identical with the on-state of an n-type device and vice versa, all assuming identical but with, where appropriate, sign reversed characteristics. In reality the electron and hole mobilities are rarely equal in an arbitrarily chosen system. Instead, one is often significantly higher than the other. So much so that in some cases it will be hidden by the high mobility current.

To a first approximation, there are two ways to describe an ambipolar transistor, either as an n-type and a p-type device in series when recombination in the channel is strong, or as the two devices in parallel when recombination is insignificant. For two phase systems with properly separated energy bands, the parallel description works very well.

3.3 Sample Preparation

OFETs used for material characterization are frequently bottom gated and uses a highly doped silicon wafer with thermal oxide on top. A metal layer, typically gold with chromium or titanium as adhesion layer, is then evaporated onto the oxide and patterned with photo-lithography to define the source and drain electrodes. Electrodes can also be defined by a shadow mask in the evaporation step, but typical geometries are usually more easily achieved with lithography. A small area of oxide is removed by etching or mechanical means to reveal the highly doped silicon that is used as gate. On top of such pre-fabricated substrates it is then possible to spin coat a material when desired. The oxide thickness should be chosen so that the gate capacitance is sufficient and the leakage currents manageable. Typical dimensions are; oxide thickness $100nm - 300nm$, channel length $1\mu m - 100\mu m$ and channel width $> 1mm$. There are of course a great many other ways to form the basic geometry of an OFET but they will not be covered here.

CHAPTER 4

Diodes

By definition a diode is a rectifier. Very rarely is the rectifying ability per se the main goal of organic components such as light emitting diodes (LED) and solar cells but the nature of these components results in rectification. Both LEDs and solar cells as well as TOF and CELIV samples have the same geometry and comprise a carrier substrate with a bottom electrode, an organic active layer, and a top electrode (Figure 4.1).

Depending on the intended application the electrodes and active layer will be different, but from a purely electrical point of view all the components will behave similarly. Because of this, the term "diode" has, in the world of organic electronics, come to be used more as a description of the sample geometry than the actual function. Even components that have an almost symmetric i/v characteristic are frequently referred to as diodes. The functionality of this basic device geometry is governed by the injection properties of the electrodes and they thus have a lot in common with Schottky diodes. A LED has an active layer that facilitates radiative recombination while solar cells usually have a blend of materials that offers separate conduction paths for electrons and holes and thus limited recombi-

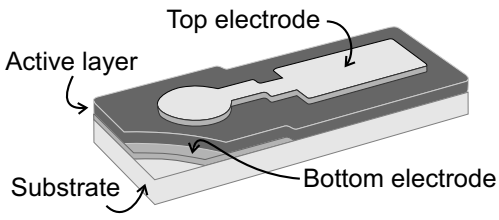

Figure 4.1. Typical organic diode.

nation. Both types of devices have one high and one low work function electrode that allows for injection and extraction of both carrier types at the appropriate electrode.

4.1 Space Charge

Space charge is due to excess charge of either sign that may exist in a medium. The frequently very low mobilities of organic semiconductors leads to an increased propensity for buildup of space charge, and in diode structures where the maximum amount of charge that can be injected or moved within the device is given by the geometric capacitance of the sample, it is easy to reach the space charge limit in monopolar applications. Sometimes space charge can be useful. In devices where only one type of carriers exists, for instance due to selective injection, the total amount of charge is known, and it is possible to extract mobility from space charge limited currents (SCLC), where a square dependence on voltage is predicted. [15] In solar cells, it is entirely negative with space charge since it limits the internal field that extracts the photo-generated carriers and increases the probability of recombination.

Most organic semiconductors have a relative dielectric constant of 3 or slightly above. With an active layer thickness of $100nm$ and a site density of $10^{26} - 10^{27} sites/m^{-3}$ the space charge limit equals about 10^{-4} carriers per site and volt.

4.2 Time of Flight (TOF)

Time Of Flight is one of the most established experimental techniques for mobility measurements. Although there are several variants, this discussion will be limited to current mode TOF with carriers generated from light excitation. In the field of organic electronics this is by far the most common type of TOF in use. For this kind of TOF measurements the investigated material is sandwiched between two electrodes, at least one of which need to be transparent, and a light pulse is used to generate carriers at the transparent electrode while a DC bias is applied to the electrodes. The generated carriers then drift through the sample generating an offset current that are monitored on an oscilloscope. The sample geometry is basically the same as that of light emitting diodes and solar cells. A schematic picture of a TOF measurement is shown in Figure 4.2.

The main differences between a TOF sample and a device such as a solar cell is that both electrodes need to be blocking and the active layer needs to be optically thick. Preferably the electrodes should be blocking for both holes and electrons since it is then possible to measure on both polarities by simply applying the appropriate bias and have the selected carriers drift through the sample. The carrier type not being measured is rapidly extracted at the electrode on the carrier generation side. As soon as carriers start reaching the opposite electrode the displacement current starts to drop off. If the sample is much thicker than the carrier generation depth a uniform mobility gives a very rapid drop and the time between the excitation and this drop gives the mobility. If the sample is thin there

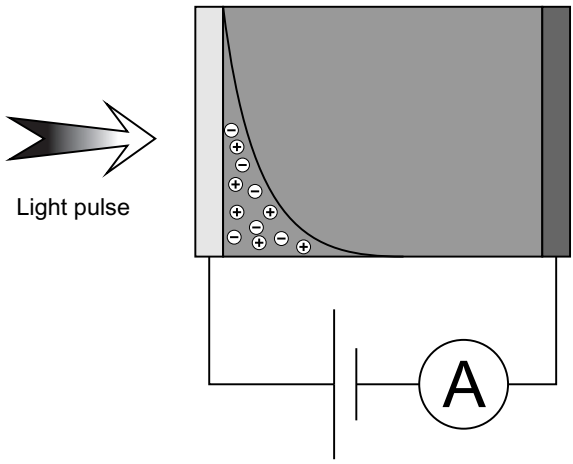

Figure 4.2. Typical TOF measurement.

will be a spread in transit times as the carriers have different distances to travel to the opposite electrode and there will be no well defined transit time. A sample can also be too thick; the transit time needs to be shorter than the carrier life time and the total measurement time needs to be shorter than the dielectric relaxation time of the material.

Out of tradition TOF retains a strong position as the benchmark experiment for charge transport but the reality is that while still being a very strong tool that gives a lot of information in a single transient, it is not very suitable for quick and easy experiments and the amount of material that is needed to make a sample is quite high. As such, it is losing out to simpler techniques such as CELIV, FET and SCLC that are more compatible with conjugated polymers.

4.2.1 TOF and GDM

The GDM implies that a propagating carrier packet has a Gaussian spatial spread. As a first order approximation the resulting spread in transit time is given by Equation 4.1, where Δt_{tr} is the spread in transit time, t_{tr} the transit time and U the potential over the sample.

$$\frac{\Delta t_{tr}}{t_{tr}} = \sqrt{\frac{2kT}{eU}} \tag{4.1}$$

It turns out that real transients often have a much larger spread than this and there are several reasons why. Equation 4.1 assumes validity of the Einstein relation and that is not necessarily true [24]. It also assumes that there is no spread to begin with, which is also wrong in most cases. Suffice to say; there is usually a spread in transit time that is much larger than predicted, but is still dependent on the actual transit time as predicted by Equation 4.1. Other disorder

dependent expressions for the spread in transit time are available [4] but these will not be treated here.

4.2.2 Dispersive Transport

In some cases the shape of the transient is independent of electric field and sample thickness, which is clearly at variance with Equation 4.1. This type of universality of the transients has traditionally been considered incompatible with a propagating Gaussian packet and labeled dispersive transport. [27] Dispersive transport occurs when there is a very high probability for carriers to be trapped for an extensive period of time at the point of generation. The result is that instead of propagating, the center of the Gaussian distribution remains stationary while the width increases. Instead of extracting all of the carriers within a limited time as normal, carriers subject to dispersive transport are extracted continuously after the first have arrived at the extracting electrode. Due to the heavy trapping the current is decreasing with time even before the first carriers reach the extracting electrode and after extraction has begun the current drops off even faster. A small shoulder can sometimes be observed when carriers begin to get extracted but frequently no features can be seen on the transient using linear scales. On logarithmic scales it is possible to see the change in current drop-off rate and, for want of any other identifiable feature, this is then frequently used to define the transit time, but instead of a measure of the average carriers transit time this is instead a measure of the transit time of the fastest carriers, which are merely a small minority and may not be representative of the material but rather the specific sample. There are several ways to identify dispersive transport. Apart from the universality feature, the slopes before and after the transit time on a logarithmic plot will be related as $-[(1+\alpha)+(1-\alpha)] = -2$, where $1+\alpha$ is the slope before, and $1-\alpha$ is the slope after the transit time. Mobility measurements based on dispersive transients are of very limited use, but it is always useful to know whether a material is subject to dispersive transport or not. It should be pointed out that universality does not necessarily mean dispersive transport and in fact many of the features of dispersive transport are possible to rationalize for normal conditions. The crossover from non-dispersive to dispersive transport is disorder dependent and thin samples with a high disorder are most likely to be dispersive. This description, unfortunately, fits many of the conjugated polymer systems.

4.3 Charge Extraction by Linearly Increasing Voltage (CELIV)

Charge Extraction by Linearly Increasing Voltage, or CELIV, is a measurement technique that is steadily gaining popularity in the field of organic electronics. [11] It is done on a semiconductor film sandwiched between two blocking electrodes in a normal diode configuration, and this is very similar to the structures used for the more traditional TOF measurements. By applying a linearly increasing voltage

to the sample, a current response comprising a capacitive part and an extraction current is obtained. From such a current transient it is then possible to calculate various quantities. A big advantage over TOF is that the electrodes do not have to be transparent and that the semiconductor layer can be much thinner since there is no need to have an optically thick sample with a carrier transit time much longer than the carriers' energetic relaxation time. This means that it is usually possible to do CELIV measurements on reverse biased solar cells or LEDs, which gives a very direct mobility measurement for the particular application. The biggest drawback is that there is no way of distinguishing holes and electrons in ambipolar systems and that the range of measureable mobilities is limited. There also need to be a sufficient amount of free carriers available in the semiconductor. Conjugated polymers with absorption in the visible range have large band gaps and the number of thermally excited carriers is usually not sufficient for measurable signals in an intrinsic material; there is also a need for some sort of doping. Whatever impurities are left from the synthesis is enough for many polymers, but the amount and type of impurities are very dependent on the type of synthesis and the purification. If there are too few carriers available it is possible to use light to excite more. This can be either in the form of continuous illumination or a short light pulse before the extraction. When a light pulse is used the measurement is designated as photo-CELIV. A calculated CELIV transient is shown in Figure 4.3 and the insert shows the extraction voltage. Both holes and electrons are present with one of the mobilities 10 times larger than the other. There is no obvious way of determining which mobility is the fastest without supplementary measurements. The relationship between a peak maximum and the associated mobility is given by Equation 4.2, where t_{max} is the peak position, d the sample thickness, μ the mobility and A the voltage rise speed. All free carriers are extracted after the slowest carriers' transit time, t_{tr}. A schematic picture of a CELIV measurement is shown in Figure 4.4.

$$t_{max} = d\sqrt{\frac{2}{3\mu A}} \tag{4.2}$$

4.3.1 Photo-CELIV

Photo-CELIV is an extension to the regular CELIV method where a light pulse precedes the carrier extraction in order to increase the carrier concentration. While CELIV only probes equilibrium carriers, photo-CELIV can be used, voluntarily or involuntarily, to probe the energetic relaxation of the photo generated carriers. In samples where the transit time is smaller than, or comparable to, the extraction time it is possible to follow the relaxation process by varying the delay time between light and extraction. [17] By calculating the number of extracted carriers as a function of delay time between light pulse and extraction, it is also possible to estimate the carrier life time. The loss of carriers can be either from recombination or via deep trapping. For materials where the loss of carriers is predominantly from recombination, a recombination constant can be calculated.

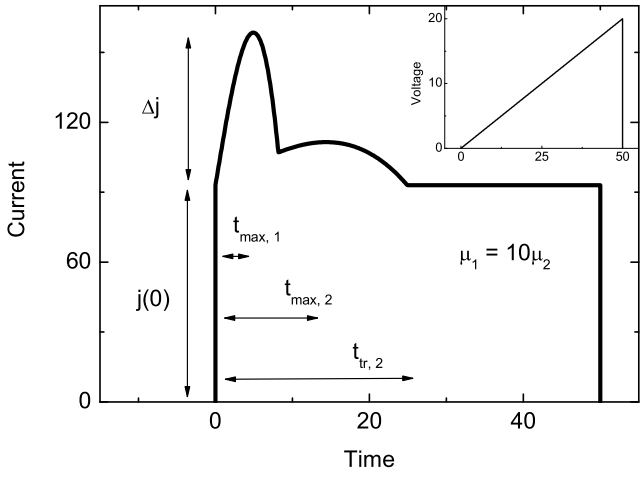

Figure 4.3. Calculated CELIV transient.

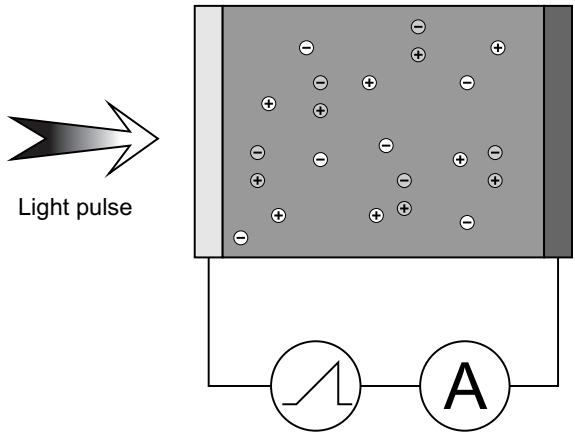

Figure 4.4. Typical CELIV and photo-CELIV measurement, the white carriers indicate equilibrium impurity generated carriers and the shaded carriers indicate the additional photo-generated carriers in photo-CELIV. Light pulse only present in photo-CELIV.

4.3.2 Built-in Potential

Very few, if any, samples have completely symmetric electrodes with a work function that matches the Fermi level of the semiconductor. The rest have a built in field or at the very least some band bending at the contacts. There is very little to do about band bending and the influence is probably minor as long as the sample is not extremely thin. Any built in fields must, however, be compensated for. The available theories on the subject of built in potentials in organic diodes are somewhat lacking, especially for two-phase systems and it is therefore much better to base any compensation on some direct measurable such as the V_{OC} of a solar cell. For photo-CELIV it is possible to obtain the optimum value by minimizing the photocurrent of the light pulse. Sometimes injection starts at a voltage lower than the offset potential and this may or may not be a problem depending on the material. The extraction current is much larger for a fully compensated device but other compensation voltages should still give the same mobility.

4.3.3 Measurement Range

The range of mobilities that can be resolved with CELIV is dependent on the sample geometry and bias range. There are many degrees of freedom in the measurements and choice of materials, but some sort of limits are nonetheless imposed by the ramp duration and the circuit RC time constant. Clearly, a mobility low enough so that it would generate an extraction maximum after the end of the extraction pulse is not easily measured. The lower limit is bias dependent but since both the extraction time and the signal amplitude are proportional to the ramp speed there is still a practical limit somewhere around $10^{-5} - 10^{-6} cm^2 V^{-1} s^{-1}$. Low conductivity materials have an extraction peak of a smaller magnitude than the capacitive response. If the extraction maximum of a small peak is close to the circuit RC constant it is also hard to detect, and this gives an upper limit to measureable mobilities. The dominant capacitance of the circuit is usually that of the sample and the relevant resistances are the measurement resistance and the sample contact resistance. Also here, there is a fair amount of freedom in choosing sample geometry and measurement resistance but again there is a trade-off with signal amplitude. Typical values are a $1.2nF$ sample capacitance, a 100Ω sample contact resistance and a 50Ω measurement resistance, which gives an RC constant of $180ns$ and consequently a high mobility limit around $10^{-3} cm^2 V^{-1} s^{-1}$. From experience it can be said that the practical limits are a bit narrower. Especially low mobilities are hard to evaluate since the peaks are very flat and have a maximum near the end of the extraction pulse. The relationship between extraction pulse length and extraction maximum of a typical sample for different mobilities is shown in Figure 4.5. The maximum ramp amplitude is fixed, $j(0)$ is the purely capacitive current response and the 1% and 70% lines indicate these respective peak positions on the extraction pulse.

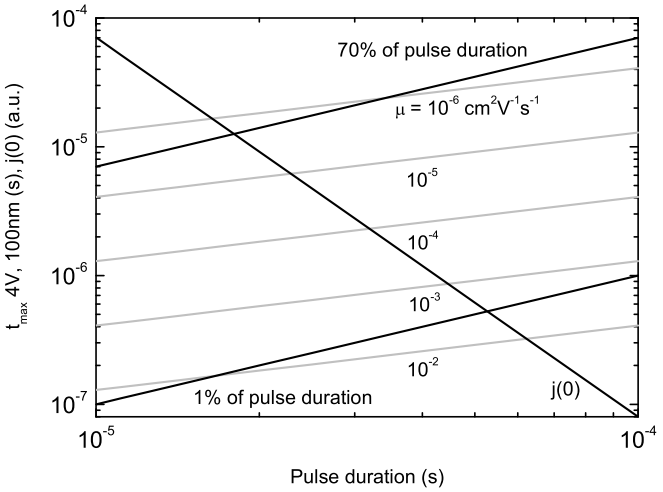

Figure 4.5. CELIV measurable mobility range, t_max as a function of pulse duration and carrier mobility. The 1% and 70% lines are the resolvable limits, and $j(0)$ gives an indication of the size of the signal

4.3.4 Ambipolar Materials

Both holes and electrons generate extraction currents in ambipolar materials, however two peaks are rarely observed in experiments. Theoretically there are two distinguishable maxima if there is more than approximately a factor of 3 in difference between the hole and electron mobility. Disorder and carrier trapping in the semiconductor and the presence of measurement noise probably increases the required mobility difference significantly and it is not unreasonable to think that a factor of 10 is closer to reality. Figure 4.6 shows the peak separation in terms of the first peaks extraction maximum as a function of mobility ratio. One thing to keep in mind is that the experimental peak positions will be influenced by each other's presence; at certain separations there can be close to a 20% difference between real and calculated mobility. The underestimate of the fast mobility as a function of mobility ratio is shown in Figure 4.7.

A reasonable assumption for an intrinsic material is that there are equal numbers of free electrons and holes. This is especially true for photo-CELIV where excess carriers are generated in equal amounts from the light pulse. The time integral of both extraction peaks should be the same and fast mobilities thus give sharper peaks of a higher magnitude than slower mobilities. When the difference in mobility is large and the conductivity low, it can be difficult to pick up the slow peak as it has much lower amplitude. A mobility ratio of 100, for instance, has a peak amplitude difference close to 10. All in all it is thus likely not possible to

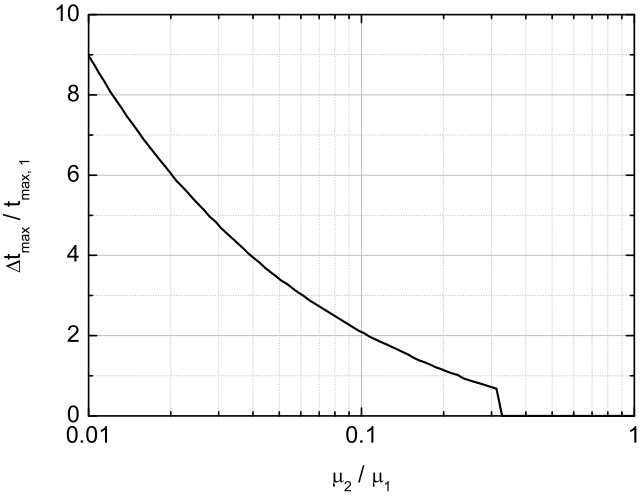

Figure 4.6. Ambipolar CELIV peak separation as a function of mobility ratio.

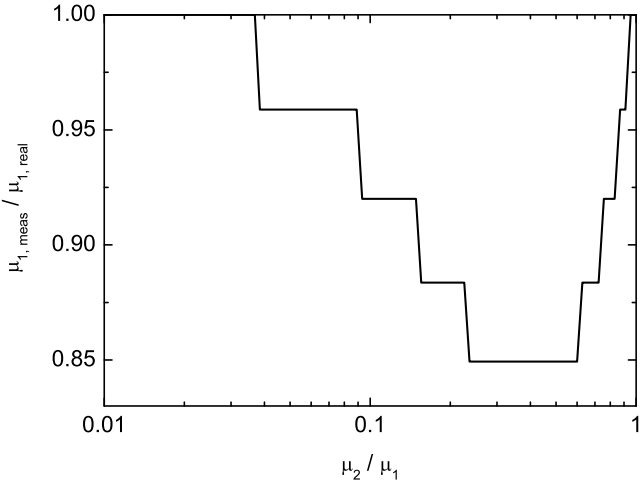

Figure 4.7. CELIV fast mobility error as a function of mobility ratio.

detect two peaks when the difference in mobility is less than a factor 10 or more than a factor 100, which is a quite narrow window.

4.4 Sample Preparation

There are many ways to build the diode structure that all have their advantages and disadvantages in various applications. Arguably the simplest way to produce a diode in a laboratory setting on a small scale is to use Indium Tin Oxide (ITO) coated glass as substrate and transparent bottom electrode and an evaporated metal top electrode with a spin coated polymer active layer in between. Processing is then limited to spin coating and metal evaporation, both of which are well established techniques with high reproducibility. Depending on the intended use of the sample, additional layers can be added between the electrodes and the active layer. For solar cells and LEDs a poly(3,4-ethylenedioxythiophene) (PEDOT) layer is usually spin coated on top of the ITO, and a Lithium Fluoride (LiF) layer evaporated on the active layer before the metal. The PEDOT enhances hole injection/extraction and the LiF enhances electron injection/extraction.

CHAPTER 5

Solar Cells

There are many ways to make use of solar energy. In fact most of the energy used today is in some sense originating from the sun. Fossil fuels, for instance, consist of organic matter, which at some point in the distant past was growing while sustained by the sun. Slightly more direct is when sunlight is used to directly produce electricity in solar cells. Silicon based solar cells have been around for a long time and are commercially available in a multitude of variants but cost prevents them from becoming the dominant source of electricity. Organic solar cells are less efficient than most of their silicon based brethren, but they are also conceivably much cheaper, which might make them a better alternative.

5.1 Performance Measures

The amount of energy that can be extracted from a solar cell is obviously limited by the solar irradiance. Depending on where and when the measurement is done there are significant variations in irradiance and to be able to compare devices under similar conditions a standard spectrum has to be used. For earth based devices this is the AM1.5 spectrum shown in Figure 5.1, which is based on light that has passed through 1.5 times the atmosphere thickness and with the composition of the atmosphere specified. The total irradiance under AM1.5 is $1000W/m^2$. To characterize the efficiency of the solar cell the following quantities are useful:

5.1.1 Power Conversion Efficiency (PCE)

The ratio of output power to incident power. This is the most important parameter as this indicates how efficient the device is under operating conditions. The

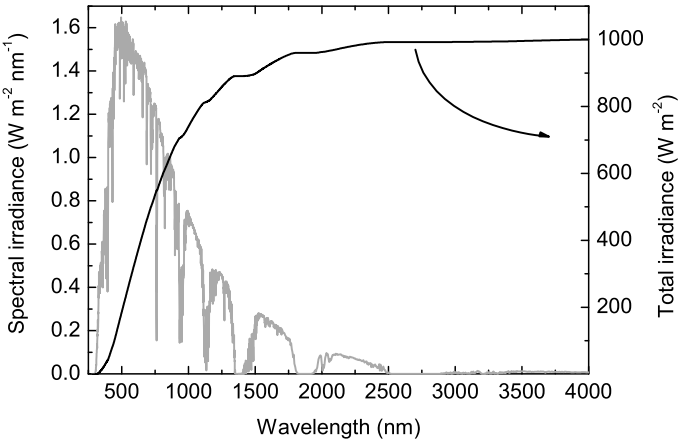

Figure 5.1. AM1.5 solar spectrum and integrated total irradiance per wavelength.

thermodynamic limit is close to 90%, but a more practical limit is that of single band gap material, which is 33%.

5.1.2 External Quantum Efficiency (EQE)

The ratio of collected charge to incident photons. There is also an internal quantum efficiency which is the ratio of generated charge to incident photons at the active layer. Quantum efficiency describes how well the solar cell can convert photons to charges. A device can have a quantum efficiency above 1 if one photon is capable of generating several excitations but this is rare.

5.1.3 Open Circuit Voltage (V_{OC})

Not surprisingly the open circuit voltage of the solar cell. This is the maximum voltage that the solar cell can supply and is limited by the built in potential of the device.

5.1.4 Short Circuit Current (J_{SC})

Again, not very surprisingly, the short circuit current of the solar cell. This is the maximum current that can be generated and is limited by the solar irradiance.

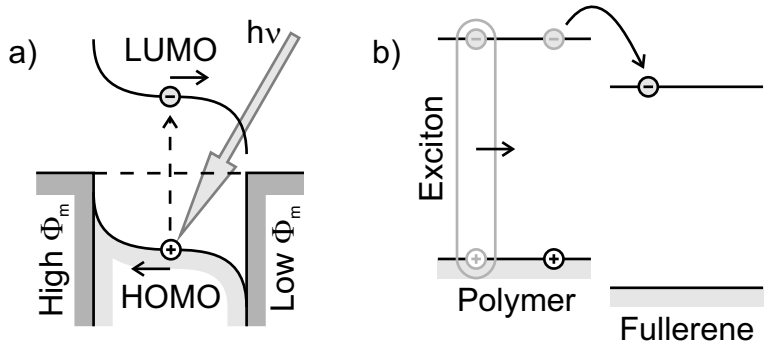

Figure 5.2. Basic solar cell working principle with exaggerated band bending, a) and exciton dissociation mechanism, b).

5.1.5 Fill Factor (FF)

This is the ratio of maximum obtained output power to the product of V_{OC} and J_{SC}. The fill factor is a measure of how close the solar cell is to an electrically ideal component and has a maximum of 1.

5.2 Working Principle

The basic function of a solar cell is convert photons into electrons and holes, which should then be harvested in such a way as to allow current to flow in an external circuit. Charges are produced when a photon is absorbed and an electron is excited to a higher energy. An absorbing material sandwiched between two electrodes with different work function producing an internal field, should thus be able to produce and extract charges from incident light as long as one of the electrodes is transparent to allow light into the device. This is schematically shown in Figure 5.2a.

5.2.1 Light Absorption

Not all incident photons are absorbed in the active layer. The semiconductor needs to have a significant band gap in order to generate power and only photons with an energy above the band gap can potentially be absorbed. Losses can also occur due to reflection before the active layer or an insufficient extinction coefficient. Various schemes of light in-coupling can be used to minimize losses. More photons are generally absorbed in materials with lower band gaps but the excess energy of shorter wavelength photons is wasted so there are practical limits on how small the band gap should be. [25] Crystalline silicon has a band gap of $1.1eV$. Most polymers have a slightly higher band gap, usually around $1.5-2eV$. The optimum band gap size depends very much on which additional energy loss mechanisms that are present in the system. A single band gap device has an efficiency limit of around 30% and in order to increase that number, multiple band gaps have to be utilized.

5.2.2 Charge Separation

When an electron in a semiconductor is excited by a photon, the resulting electron hole pair is electrostatically bound together and some energy is needed to break them apart. The bound electron-hole pair is a quasi particle called an exciton and can diffuse through the semiconductor, recombine radiatively (photoluminescence) or non-radiatively, or separate into free charges. An exciton in an extended state material has a fairly small binding energy, typically $10meV$, and is sometimes referred to as a Mott-Wannier exciton. These can be separated very easily and it is usually enough with the built in field of a solar cell to get sufficient charge separation. Polymers, which are localized state materials, yield much more tightly bound excitons, frequently with binding energies on the order of $1eV$ and these are sometimes referred to as Frenkel excitons. Because a bit more effort is required to separate Frenkel excitons they are more long lived and materials in which they occur are thus considered excitonic materials. Polymers are usually excitonic materials. The solution to obtaining efficient charge separation in excitonic materials is to use two-phase systems, where the two phases have different electronegativity and ionization potential so that charge separation occurs through transfer of the excited electron to the more electronegative phase or through transfer of the hole to the phase of lower ionization potential (Figure 5.2b). Some of the carriers' energy is lost due to the charge transfer, and instead of the band gap it is then the HOMO level of the electron donor phase and the LUMO level of the electron acceptor phase that limits the energy of the extracted carriers.

5.2.3 Charge Transport

After the charges are generated they must be transported to the appropriate electrode in order to contribute to the power output of the solar cell. There is always a risk of recombination or trapping of the photo-generated charges and in order for a solar cell to be efficient, the carriers must be fast enough to reach the electrodes before recombination occurs.

The maximum thickness, d, of a device in which carriers move through drift, that allows collection of all carriers, is given by Equation 5.1, where μ is the mobility, τ the carrier lifetime and E the electric field.

$$d = \mu\tau E \tag{5.1}$$

Reasonable numbers for many materials might be $d = 100nm$, $\tau = 10^{-6}s$, $\mu = 10^{-5}cm^2V^{-1}s^{-1}$ and a built in potential of $1.3V$. On an order of magnitude scale, these numbers indicate that Equation 5.1 might well impose a limit on real devices. A material with an absorption onset at $700nm$ and which absorbs every photon of higher energy is theoretically capable of generating around $20mA/cm^2$ of photo-current. Figure 5.3 shows the maximum photo-current possible to generate at different loads, based on Equation 5.1, assuming a uniform field and carrier distribution, and ideal electrical behaviour. Rough estimates of the fill factor of ideal devices for the different parameter sets are also shown. It is entierly possible for a poorly performing device with, for instance, extensive recombination, to have

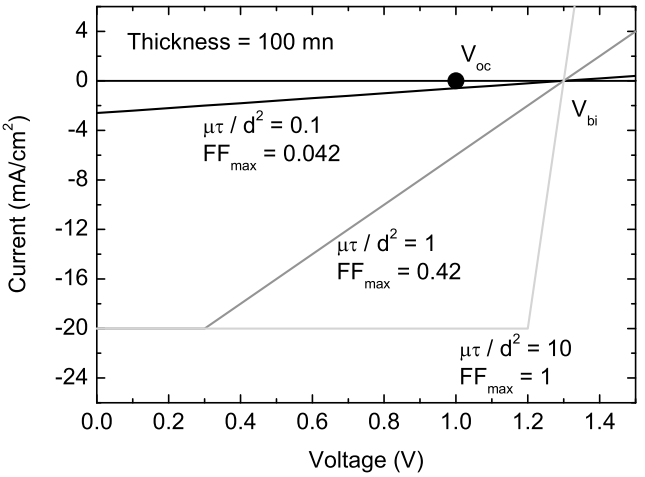

Figure 5.3. Approximate FF and J_{SC} for an electrically ideal solar cell for different device and material parameters.

a higher fill factor, but the current would then be reduced compared to the ideal case. The black line corresponds to the values given above.

Usually, the light intensity from the sun is low enough, so that space charge effects can be neglected. A more than worst case scenario can be found in Figure 5.4, where the required mobility to avoid space charge as a function of absorption onset for a $100nm$ thick solar cell with a built in field of $1V$ that absorbs every photon with an energy above the band gap is shown. Only one type of carrier is assumed to be generated, and all of the carriers are also assumed to be generated at the electrode opposite to where they are collected. If the lowest mobility is above $10^{-4}cm^2V^{-1}s^{-1}$, space charge will obviously never be a factor but for low band gap materials with low mobilities there might be a problem.

The carrier concentration in a solar cell is usually too low for carrier concentration to have a significant impact on mobility. A reasonable value for site density in a polymer is somewhere in the range $10^{26} - 10^{27}sites/m^3$. In a $100nm$ thick sample absorbing every photon of sufficient energy with the absorption onset at $800nm$ and that has carrier mobilities in the range $10^{-5} - 10^{-4}cm^2V^{-1}s^{-1}$, the carrier concentration is in the range $10^{-5} - 10^{-3}$ carriers per site.

5.3 Recombination

There are several different recombination mechanisms that prevents carriers from being extracted and that thus determines the carrier lifetime. [6] [26] For organic solar cells the following are the most relevant:

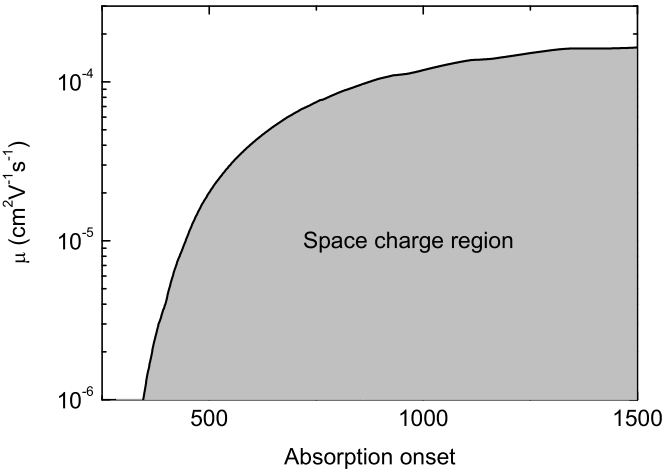

Figure 5.4. Integrated AM1.5 solar spectrum normalized to mobility space charge limit through geometric capacitance and maximum carrier drift time.

5.3.1 Geminate Recombination

Recombination between the electron and hole originating from the same excitation. Geminate recombination is usually quite strong in pure polymers where excitons are very long lived but is suppressed in blends.

5.3.2 Monomolecular Recombination

Recombination through defects. The recombination rate is proportional to the defect density and carrier concentration of the appropriate type.

5.3.3 Bimolecular Recombination

Radiative or non-radiative. Conduction band electron with valence band hole. For pure polymers bimolecular recombination is usually of Langevin type, where it is controlled through the faster of the participating mobilities and is proportional to Equation 5.2 where e is the elementary charge, ϵ the absolute permittivity and μ_n and μ_p the mobility of electrons and holes respectively. Blend systems, however, facilitates different percolation paths and bimolecular recombination is thus suppressed. [14]

$$\beta_L = \frac{e}{\epsilon}(\mu_n + \mu_p) \tag{5.2}$$

5.3.4 Recombination in Solar Cells

A photo-generated exciton can recombine geminately. After dissociation the carriers can recombine geminately with each other, monomolecularly through recombination centres, or bimolecularly with another carrier generated elsewhere. In two phase systems such as bulk heterojunction solar cells there is a significant driving force for charge separation at the interfaces and transport of the carriers occurs in spatially separated phases, which strongly limits bimolecular and geminate recombination, as long as there is a junction within the exciton diffusion length of the excitation. Carrier concentrations under relevant light intensities are also quite low, which further limits bimolecular recombination. It is thus reasonable to suspect that the main recombination should be monomolecular and that the carrier lifetime, and thus performance, is limited by recombination centers in the form of impurities and defects. It is also, of course, possible to consider geminate recombination of free carriers as well, but degradation of device performance seems to suggest that the mobility stays more or less constant in a degrading device. This means that if the morphology is stable, recombination must be increasing, and since morphology and carrier concentration are constant, the recombination must be monomolecular. In reality these assumptions might not be true for all materials.

CHAPTER 6

Force Microscopy Based Electrical Measurements

Some scientific effort is directed towards producing conductive and semi conductive fibers with very small dimensions, which are necessary to characterize. Ordinary electrical characterization techniques are usually too crude to give any information on individual fibers so alternatives have to be found. Some such alternatives can be found in force microscopy. It is well beyond the scope of this dissertation to treat force microscopy with any thoroughness but a short introduction to the different modes pertaining to electrical measurements will be given.

6.1 Force Microscopy

Atomic Force Microscopy (AFM) is a type of scanning probe microscopy that utilizes a small cantilever to probe surfaces through deflection forces. The resolution is very high and it is even possible to resolve individual atoms in periodic lattices if the conditions are favorable. It is also possible to press down with the cantilever so that a contact to the substrate is achieved and to use metal-coated cantilevers to get electrical information about the sample. By biasing the cantilever it is thus possible to use the cantilever as an electrode in contact mode or to read out the local surface potential through electrostatic interactions. Direct current measurements are labeled Conductive-AFM and surface potential measurements Kelvin Force Microscopy (KFM).

6.1.1 Conductive-AFM

Modern instruments frequently have the ability to sweep the potential of the cantilever and / or the sample holder and are thus able to do i/v-characterization. It is also possible to use external equipment for the electrical measurements and only

use the AFM as a contacting tool. A complete conductive-AFM scan of a surface gives simultaneous topographical and electrical information for every pixel in the measurement. The drawbacks are that the conductivity of the sample needs to be fairly high to be possible to measure, that the cantilever can damage sensitive samples and that current injection from the cantilever can be problematic (See Section 2.4).

6.1.2 Kelvin Force Microscopy (KFM)

KFM measurements are performed in non-contact mode and either natural surface potential variations in the sample or the distribution of applied potentials are measured. [19] Since only potential is measured the conductivity requirements are much lower than for conductive-AFM. Drawbacks are that no actual quantitative information can be gained and that the measurement is inherently integrating so that the resolution is limited. A complete KFM scan gives simultaneous information about topography and potential for every pixel in the measurement.

6.2 Sample Preparation

The cantilever makes up one electrode in the electrical AFM measurements but two electrodes are required for current measurements in conductive-AFM, and one or more electrodes are needed to supply potentials for KFM measurements. It is in theory possible to use lithographically predefined patterns but in reality the contact between such patterns and sample fibers are poor, and solution processed fibers tend to have an affinity for either the electrodes or the substrate, which makes it hard to get an appropriate configuration of fibers and electrodes. Instead it is usually necessary to evaporate electrodes on top of fibers distributed over a substrate. There are two fairly simple ways to achieve this on a scale suitable for AFM-based measurements; wire masks and tilted evaporation.

6.2.1 Wire Masks

It is unfeasible to produce reusable masks on the micrometer dimensions necessary for use in AFM studies. The simplest way is to use a thin monofilament, which is attached to one end of the substrate and weighted down with a small mass at the other end while it is fixated in the desired position by an adhesive such as glue (Figure 6.1). Although quick and easy, this method does not produce very well defined electrodes. Figure 6.2 shows a topographical and potential image of an electrode pair produced with a wire mask and from this data it is possible to conclude that the electrodes extend well inside the channel defined by the wire and that it is hard to determine the exact position of the electrode edges. Indeed, without the aid of the potential image it would be almost impossible to define the electrode edges. As long as this problem is considered it is still a decent way of quickly producing electrodes.

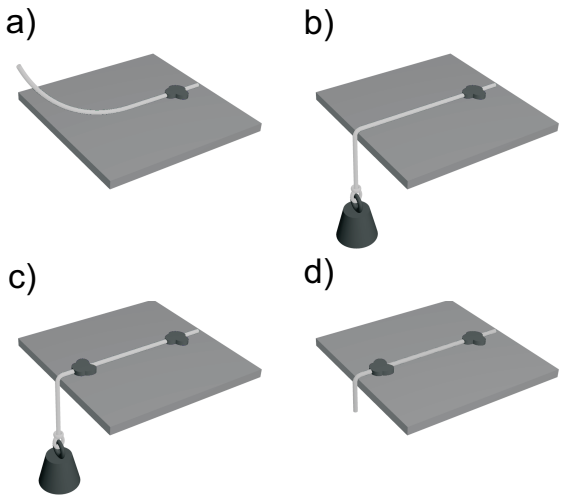

Figure 6.1. Wire mask. a) One end of the wire is attached with glue, b) a small mass is attached, c) the other end of the wire is attached with glue, and d) the mass is removed.

6.2.2 Tilted Evaporation Masks

When sharp edges are important, for instance when low conductivity materials need to be probed in the immediate proximity of a well defined electrode, it is possible to use a piece of newly cracked crystalline silicon as mask. Given sufficient proximity between the mask and the substrate a very sharp electrode edge will be produced that is suitable for, for instance, conductive AFM. It is also possible to use a thick electrode produced in this way as an evaporation mask for a second electrode by tilting the substrate during the evaporation of the second electrode (Figure 6.3). This produces electrodes with a typical separation of 100 nm. Figure 6.4 shows an AFM picture of an electrode evaporated using a piece of newly cracked crystalline silicon as mask.

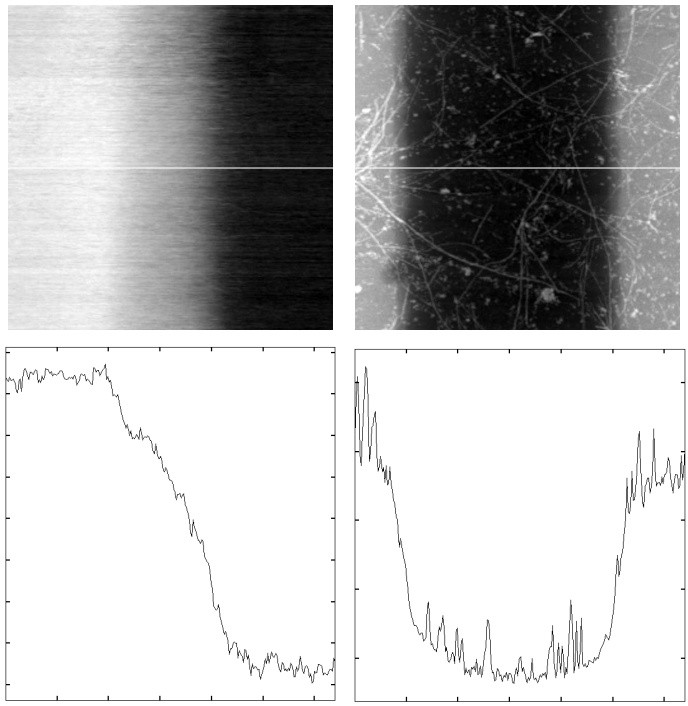

Figure 6.2. Potential (left) and topographical (right) data of the same $6.4 \times 6.4 \mu m$ area. There is a $2V$ difference in potential between the electrodes and they are $30nm$ thick.

Figure 6.3. Tilted evaporation. a) After the first evaporation step with silicon mask still in place, b) Sample position and secondary mask during the tilted evaporation step, and c) finished result.

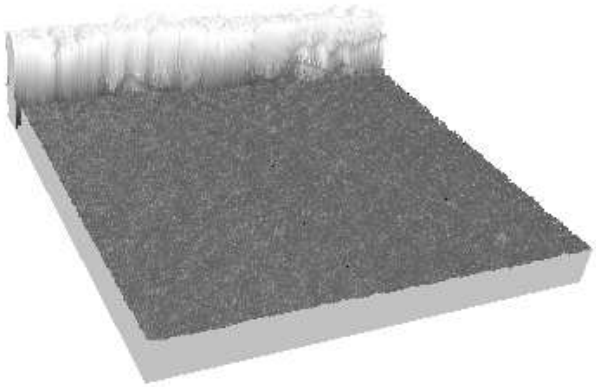

Figure 6.4. Gold electrode evaporated on SiO_2 with a newly cracked silicon mask. The area is $748 \times 748nm$ and the thickness of the electrode is $25nm$.

CHAPTER 7

Scientific Results

7.1 Bias Stress and Hysteresis

There is always a difference between the sweep directions in a cyclic transfer characteristics measurement on an OFET. Often this is due to bias stress and is referred to as hysteresis. It is possible to influence the magnitude of the hysteresis in many ways, both measurement wise and with atmospheric and ambient conditions. In Paper I hysteresis is explained as a non-equilibrium effect. In essence, the reason for this is the small DOS and low mobility of polymers. As is evident from Equation 2.3, there is an exponential decrease in carrier jump probability when the target site is at a higher energy. The small DOS and concomitant high carrier concentrations render many of the carriers at the lowest energies immobile because neighbouring sites of suitable energy are occupied and the penalty for reaching sites at higher energies are too severe. When the channel is formed, equilibrium has not yet been reached and most carriers are free to move, but as equilibrium is approached more and more carriers becomes immobile.

The main strength of this theory compared to the other suggestions that has been presented in the literature is that it is consistent with all experimental observations and not just a subsection, as is usually the case. One example of this is the notion of carrier trapping by defects. The release time of a carrier trapped at some trap level should decrease with temperature. It is thus reasonable to conclude that the hysteresis should decrease with increasing temperature but this is not the case and the reason is that the approach to equilibrium is faster at elevated temperatures.

As long as a hydrophilic gate insulator such as SiO_2 is used, water has a profound effect on device performance, especially hysteresis, which can be shown to increase with humidity (Figure 7.1). Hysteresis measurements in humid en-

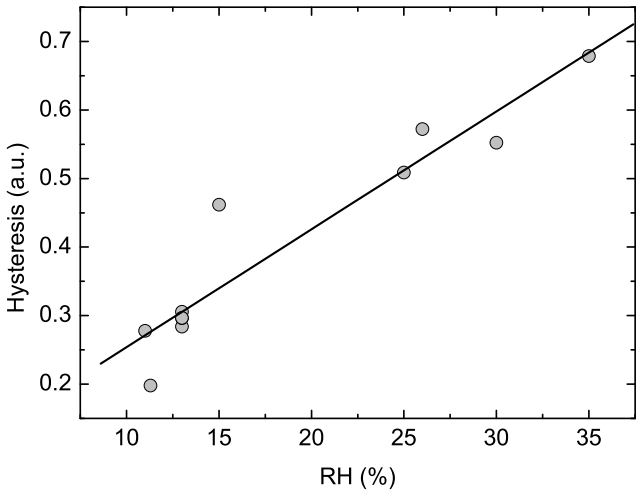

Figure 7.1. Hysteresis as a function of relative humidity. Hysteresis is calculated as the normalized current ratio of off-to-on and on-to-off sweeps at $-24V$ gate potentilal.

vironments might thus show erroneous temperature dependence since water will evaporate as the temperature is increased and thus hide the increasing hysteresis.

Most probably, water adds disorder to the system and a mobility versus temperature measurement that is done in a humid environment yields a larger σ value than a measurement in a dry environment. A sufficiently dry environment gives mobility temperature dependence data that is consistent with different measurement techniques where no hydrophilic interface interferes with the measurements, while measurements in a humid environment can result in σ values that are more than twice as large as those obtained by different methods. Unfortunately, a dry environment means ultra high vacuum (UHV, pressure $< 10^{-9} torr$), as high vacuum (HV, $< 10^{-3} torr$) still has enough water present to severely influence measurements. Above the boiling point of water there is less of a difference between HV and UHV. The difference between HV and UHV is exemplified in Figure 7.2, where both the hysteresis variation and difference in temperature dependence can be seen. It is worth to emphasize; transistor measurements done under proper conditions are, at least for the amorphous APFO polymers, fully consistent with other measurements, such as TOF, CELIV and SCLC, and with existing theory.

There may well be more than one cause for hysteresis. A very obvious case is the relationship between hysteresis and polymer HOMO that can sometimes be seen when the same electrode material is used, especially when measurements are done under moderate illumination and on fairly thick polymer films. This is due to poor injection. Equilibrium carriers in the polymer bulk are initially able to

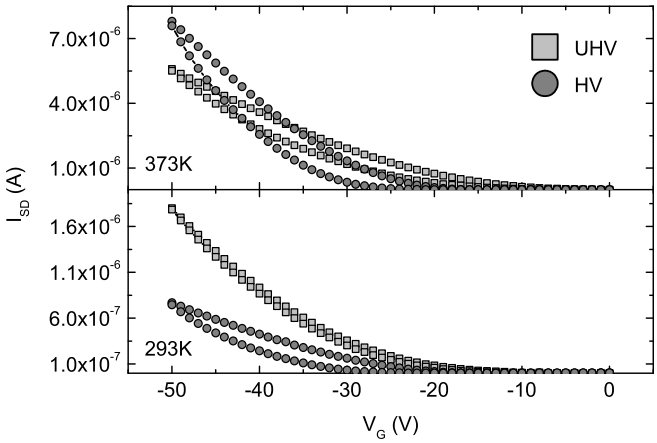

Figure 7.2. APFO-Green5 transfer characteristics taken at $293K$ and $373K$ in HV and UHV.

form a channel but injection is insufficient to sustain it at lower gate biases, when the gate-induced p-doping is small. For more on injection and why increased gate bias promotes it see Section 2.4.2. A plot of threshold shift versus polymer HOMO for a number of different polymers can be found in Figure 7.3.

7.2 TOF on APFO

A TOF transient for APFO-4 is shown in Figure 7.4. It does exhibit a shoulder on linear scales but its position is different from the inflection point on logarithmic scales. Figure 7.5 shows a series of normalized transients for different fields. The shape is universal and the slopes before and after the inflection point is consistent with an α value of 0.95 indicating dispersive transport.

At best this transient, as the high α value indicates, might be possible to evaluate in a meaningful way with a bit of error and at worst it is of no use. Either way the amount of material and effort required is rather large compared to the usefulness of the results. APFO-4 is also the polymer that, among the investigated, gives the "nicest" transients. The conclusion from this is that if alternative measurement techniques can be used it is not worthwhile to do TOF.

7.3 Solar Cell Performance

There are many parameters to optimise in organic solar cells and many of them, for instance band gap and exciton dissociation energy, involves different materials. It

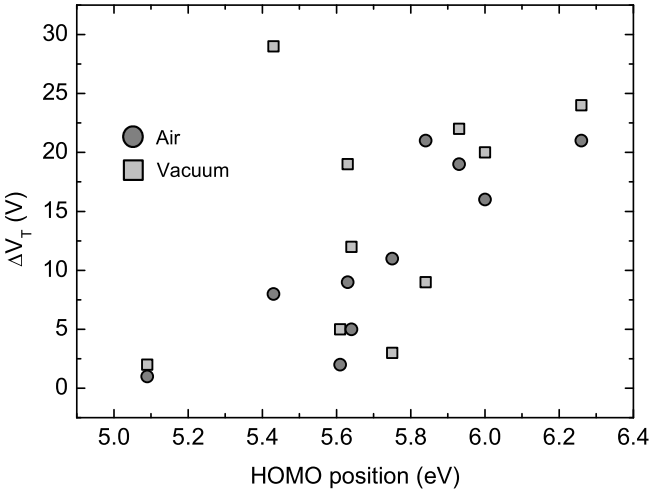

Figure 7.3. Threshold shift as a function of polymer HOMO position.

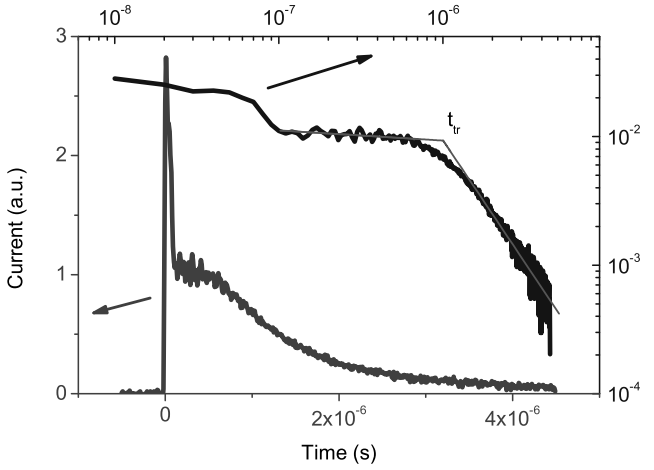

Figure 7.4. APFO-4 TOF transient.

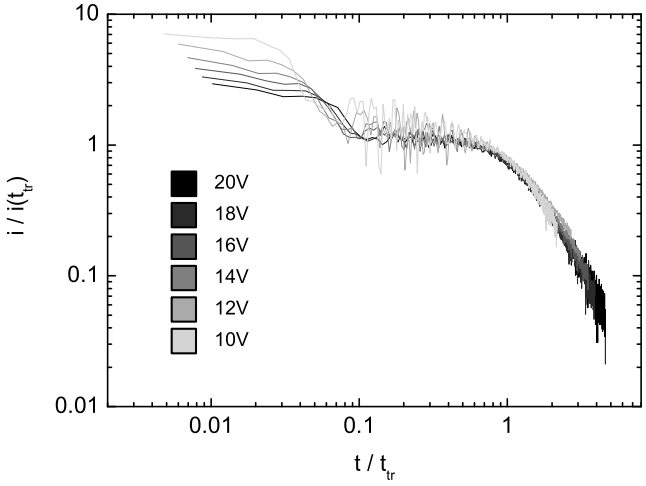

Figure 7.5. APFO-4 TOF transient universality.

is necessary to characterize new materials electrically in order to determine if they have potential for high efficiency. As per Section 5.2.3, the critical parameter is the $\mu\tau$ product. Obviously, high $\mu\tau$ products are desirable, but a low $\mu\tau$ product can also be interesting if there is possibility that it can be increased by post processing. One part of evaluating this is determining both the electron and hole mobility and comparing them with obtained values in the pure phase and in other composite systems. Figure 7.6 and Figure 7.7 shows electron and hole mobilities in two decently performing polymer systems; APFO-3:PCBM60 (Paper III) and APFO-Green5:PCBM60 (Paper II) correlated with solar cell performance. In the former it is the electron mobility that is the lowest and thus limiting and in the latter it is vice versa.

Mobility measurements on pure APFO-3 give fairly reproducible results with only small variations. Measurements on blends with different acceptors show that PCBM60 increases the hole mobility in the polymer, while other acceptors decrease it (Figure 7.8 and Paper IV). Since the amount of PCBM60 should be minimized due to the poor absorption of the compound, it can be concluded that in order to increase device performance it is necessary to find a way to increase the electron mobility while retaining the positive impact on hole mobility of the PCBM60.

Mobility measurements on pure APFO-Green5 display a much wider scatter than does APFO-3 measurements. From Figure 7.7 it is clear that hole mobility is limiting and also fairly independent on acceptor loading. Solar cells retain the big scatter in pure APFO-Green5 mobility and there are huge variations in performance for identical devices. The conclusion is thus that the reason for the

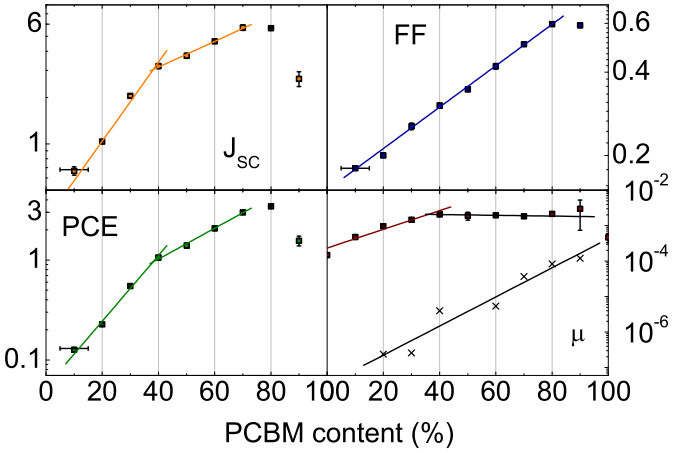

Figure 7.6. APFO-3 solar cell performance and mobility; (a) short circuit current in mA/cm2, (b) fill factor, (c) power conversion efficiency (%), and (d) FET hole mobility (squares) and CELIV electron mobility (crosses) ($cm^2V^{-1}s^{-1}$).

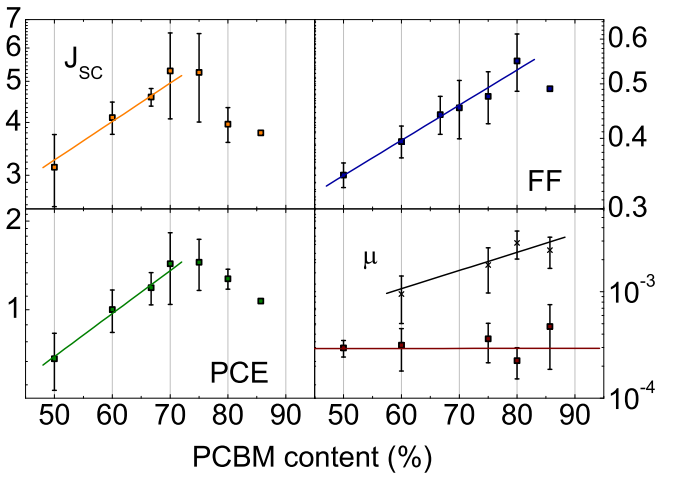

Figure 7.7. APFO-Green5 solar cell performance and mobility; (a) short circuit current in mA/cm2, (b) fill factor, (c) power conversion efficiency (%), and (d) FET hole mobility (squares) and FET electron mobility (crosses) ($cm^2V^{-1}s^{-1}$).

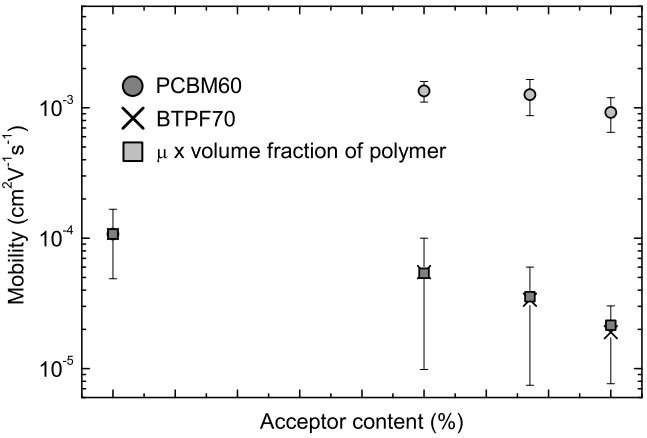

Figure 7.8. APFO-3 hole mobility as a function of acceptor loading for PCBM60 and BTPF70.

large mobility variations should be sought in order to achieve reproducibility.

Together, this and other similar data shows that transport is indeed limiting solar cell performance and is a critical parameter to consider. It is possible to see a general correlation between hole mobility and solar cell performance if many materials are considered so in a general sense it seems like the polymers, more than the fullerenes, are limiting in terms of transport. Such a correlation is not extremely strong because of all the other differences between polymers, such as absorption and HOMO / LUMO position, but it is clear (Figure 7.9).

7.4 Semiconductive and Conductive Fibers

There are many possible applications for conductive nano-wires. They can conceivably be used as current collectors in organic solar cells to get around transport limitations or they can be used as building blocks for components and as connectors in nano-electronics among other things. A nano-wire is, obviously, quite small. Electrical characterization of nano-wires is difficult for two reasons; they are small and they are small. Their small dimensions make them difficult to manipulate and contact, but it also makes for very small currents at applicable voltages. Nano-wires have been fabricated with biological templates such as DNA or amyloid fibrils that has been coated with, or has had integrated, a conductive or semiconductive polymer or oligomer. The most conductive polymer that has been used is PEDOT and while it is available in many different forms with a significant spread in optical and electrical properties it can, for the sake of this argument, be considered as having a conductivity on the order of $0.1 S/cm$. A solid PEDOT

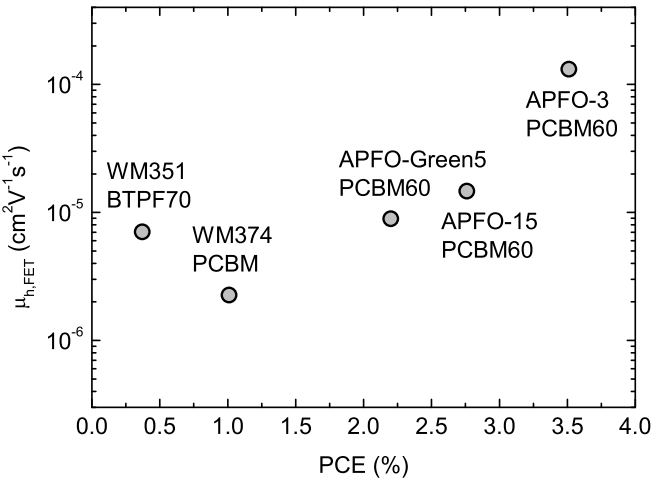

Figure 7.9. Hole mobility versus PCE for selected polymers.

fiber with a diameter of $10nm$ that is measured over a distance of $1\mu m$ at a potential of $1V$ would thus give currents on the order of $10^{-13}A$. In reality, it is not unlikely that the currents would be several orders of magnitude lower than that, due to the fact that only a fraction of the fibers actually is of conductive polymer and that many materials have a much lower conductivity than PEDOT. While still conceivably possible, direct current measurements on single fibers are not advisable. Instead KFM can be used to assign conductivity to the fibers and conductivity measurements on ensembles of fibers can be used to get approximate conductivity numbers.

It is possible to create self-assembled luminescent wires through fibrillation of bovine insulin in the presence of a luminescent oligoelectrolyte. [7] [8] These wires are relatively durable and although the oligoelectrolytes used has a low conductivity it is still interesting to investigate the potential for this type of structures in electronic applications. The fact that fibers are formed and that they are luminescent proves conceptual negotiability of the system. What is needed to warrant further investigation is an indication that the interaction between insulin and oligoelectrolyte is such that high conductivity can be expected in similar systems.

KFM images taken at different biases, along with a topographical image of insulin / oligoelectrolyte fibers in the gap between two gold electrodes on a SiO_2 substrate is shown in Figure 7.10. It is clear that the KFM images reflect local potential and that there are no significant topographical artefacts. However, a severe time dependence prohibits a unanimous interpretation of the data as displaying conductive fibers. The potential distribution on both the fibers and elsewhere

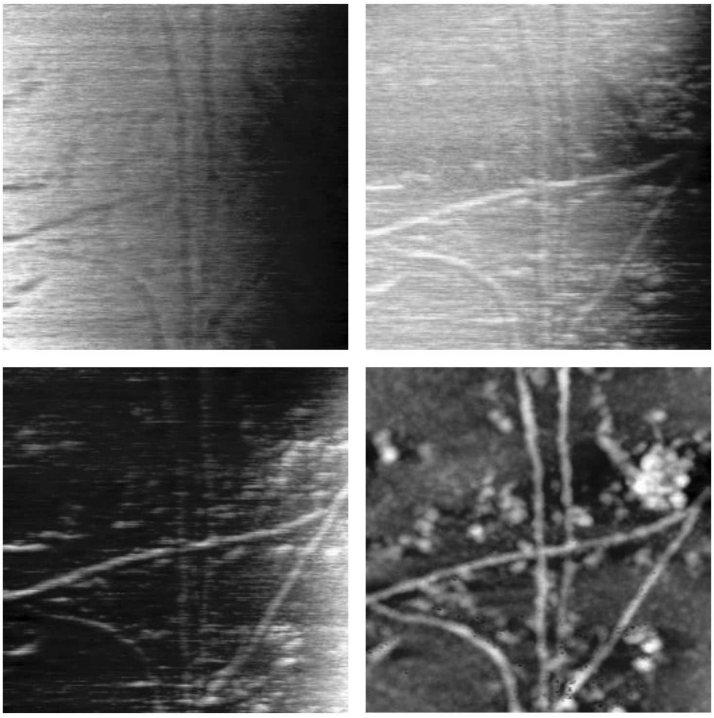

Figure 7.10. $1.52 \times 1.52\mu m$ KFM images at different bias, and topography (bottom right) of insulin / oligoelectrolyte fibers in the middle of an approximately $2\mu m$ wide gap between two gold electrodes. The fibers are approximately $6nm$ high, and the potential contrast of the fibers is about $0.2V$ at $3V$ applied bias.

shifts with time on a minute to hour timescale. One possible explanation for this is that there are ions present on the substrate surface that can move in the applied fields. This explanation is somewhat corroborated by the fact that it is possible to see contrast in the field direction that increases with time across single fibers aligned parallel to the electrodes and on small objects in the gap, which would then, conceivably, be due to ions moving on the surface and getting stuck at larger objects.

It is, nonetheless, compelling to ascribe some amount of conductivity to the fibers based on Figure 7.10, but the results are inconclusive and at best the conductivity is still extremely low, not much higher than that of the contaminated SiO_2. As a feasibility study, the results are quite encouraging. The insulin / oligoelectrolyte fibers may well be conductive and more highly conductive substitutes for the oligoelectrolyte can potentially give much clearer results. Furthermore, it has been established that KFM is a useful and suitable technique for such measurements.

Bibliography

[1] P. W. Anderson. Absence of diffusion in certain random lattices. *Physical Review*, 109(5):1492–1505, 1958.

[2] P. W. Anderson. The size of localized states near the mobility edge. *Proceedings of the National Academy of Sciences of the United States of America*, 69(5):1097–1099, 1972.

[3] V. I. Arkhipov, P. Heremans, E. V. Emelianova, G. J. Adriaenssens, and H. Bassler. Weak-field carrier hopping in disordered organic semiconductors: the effects of deep traps and partly filled density-of-states distribution. *Journal of Physics-Condensed Matter*, 14(42):9899–9911, 2002.

[4] H. Bassler. Charge transport in disordered organic photoconductors - a monte-carlo simulation study. *Physica Status Solidi B-Basic Research*, 175(1):15–56, 1993.

[5] R. Coehoorn, W. F. Pasveer, P. A. Bobbert, and M. A. J. Michels. Charge-carrier concentration dependence of the hopping mobility in organic materials with gaussian disorder. *Physical Review B*, 72(15):155206, 2005.

[6] S. De, T. Pascher, M. Maiti, K. G. Jespersen, T. Kesti, F. L. Zhang, O. Inganas, A. Yartsev, and V. Sundstrom. Geminate charge recombination in alternating polyfluorene copolymer/fullerene blends. *Journal of the American Chemical Society*, 129(27):8466–8472, 2007.

[7] A. Herland, P. Bjork, K. P. R. Nilsson, J. D. M. Olsson, P. Asberg, P. Konradsson, P. Hammarstrom, and O. Inganas. Electroactive luminescent self-assembled bio-organic nanowires: Integration of semiconducting oligoelectrolytes within amyloidogenic proteins. *Advanced Materials*, 17(12):1466–1471, 2005.

[8] A. Herland, P. Bjork, K. P. R. Nilsson, J. D. M. Olsson, P. Asberg, P. Konradsson, P. Hammarstrom, and O. Inganas. Electroactive luminescent self-assembled bio-organic nanowires: Integration of semiconducting oligoelectrolytes within amyloidogenic proteins (vol 17, pg 1466, 2005). *Advanced Materials*, 17(14):1703–1703, 2005.

[9] T. Holstein. Studies of polaron motion part i. the molecular-crystal model (reprinted from annals of physics, vol 8, pg 325-342, 1959). *Annals of Physics*, 281(1-2):706–724, 2000.

[10] T. Holstein. Studies of polaron motion part ii. the "small" polaron (reprinted from annals of physics, vol 8, pg 343-389, 1959). *Annals of Physics*, 281(1-2):725–773, 2000.

[11] G. Juska, K. Arlauskas, M. Viliunas, and J. Kocka. Extraction current transients: New method of study of charge transport in microcrystalline silicon. *Physical Review Letters*, 84(21):4946–4949, 2000.

[12] G. Juska, N. Nekrasas, K. Genevicius, J. Stuchlik, and J. Kocka. Relaxation of photoexited charge carrier concentration and mobility in mu c-si : H. *Thin Solid Films*, 451-452:290–293, 2004.

[13] G. W. Kang, K. M. Park, J. H. Song, C. H. Lee, and D. H. Hwang. The electrical characteristics of pentacene-based organic field-effect transistors with polymer gate insulators. *Current Applied Physics*, 5(4):297–301, 2005.

[14] L. J. A. Koster, V. D. Mihailetchi, and P. W. M. Blom. Bimolecular recombination in polymer/fullerene bulk heterojunction solar cells. *Applied Physics Letters*, 88(5):052104, 2006.

[15] Murray A. Lampert and Peter Mark. *Current injection in solids*. Academic Press, New York,, 1970. [ISBN] 0124353509.

[16] A. Miller and E. Abrahams. Impurity conduction at low concentrations. *Physical Review*, 120(3):745–755, Nov 1960.

[17] A. J. Mozer, N. S. Sariciftci, L. Lutsen, D. Vanderzande, R. Osterbacka, M. Westerling, and G. Juska. Charge transport and recombination in bulk heterojunction solar cells studied by the photoinduced charge extraction in linearly increasing voltage technique. *Applied Physics Letters*, 86(11):112104, 2005.

[18] A. J. Mozer, N. S. Sariciftci, A. Pivrikas, R. Osterbacka, G. Juska, L. Brassat, and H. Bassler. Charge carrier mobility in regioregular poly(3-hexylthiophene) probed by transient conductivity techniques: A comparative study. *Physical Review B*, 71(3):035214, 2005.

[19] V. Palermo, M. Palma, and P. Samori. Electronic characterization of organic thin films by kelvin probe force microscopy. *Advanced Materials*, 18(2):145–164, 2006.

[20] W. F. Pasveer, J. Cottaar, C. Tanase, R. Coehoorn, P. A. Bobbert, P. W. M. Blom, D. M. de Leeuw, and M. A. J. Michels. Unified description of charge-carrier mobilities in disordered semiconducting polymers. *Physical Review Letters*, 94(20):206601, 2005.

[21] R. Peierls. Reflections on broken symmetry. *Physics Today*, 44(2):13–, 1991.

[22] R. Peierls. Broken symmetries. *Contemporary Physics*, 33(4):221–226, 1992.

[23] Y. Preezant and N. Tessler. Carrier heating in disordered organic semiconductors. *Physical Review B*, 74(23):235202, 2006.

[24] Y. Roichman and N. Tessler. Generalized einstein relation for disordered semiconductors - implications for device performance. *Applied Physics Letters*, 80(11):1948–1950, 2002.

[25] M. C. Scharber, D. Wuhlbacher, M. Koppe, P. Denk, C. Waldauf, A. J. Heeger, and C. L. Brabec. Design rules for donors in bulk-heterojunction solar cells - towards 10 *Advanced Materials*, 18(6):789–, 2006.

[26] I. G. Scheblykin, A. Yartsev, T. Pullerits, V. Gulbinas, and V. Sundstrom. Excited state and charge photogeneration dynamics in conjugated polymers. *Journal of Physical Chemistry B*, 111(23):6303–6321, 2007.

[27] H. Scher and E. W. Montroll. Anomalous transit-time dispersion in amorphous solids. *Physical Review B*, 12(6):2455–2477, 1975.

[28] O. Tal, Y. Rosenwaks, Y. Roichman, Y. Preezant, N. Tessler, C. K. Chan, and A. Kahn. Threshold voltage as a measure of molecular level shift in organic thin-film transistors. *Applied Physics Letters*, 88(4):043509, 2006.

[29] L. Torsi, A. Dodabalapur, L. J. Rothberg, A. W. P. Fung, and H. E. Katz. Intrinsic transport properties and performance limits of organic field-effect transistors. *Science*, 272(5267):1462–1464, 1996.

APPENDIX A

Polymers and Fullerenes

A.1 APFO Polymers

APFO stands for Alternating PolyFluOrene. They are copolymers of fluorene and one or more other segments. The initial thought was that the fluorene would contribute some of the properties of its homopolymer, such as liquid crystallinity and high mobility, to the APFO-polymer, while the other segments could be used to tailor the optical properties of the polymer. Usually donor-acceptor-donor (D-A-D) segments of various kinds make up the other part of the APFO. D-A-D segments utilize electron-donating and electron-withdrawing substituents to create partial charge transfer between the donating and accepting groups along the polymer chain in order to lower the band gap. The stronger the D-A-D character, the lower the band gap gets. Both the fluorene and the D-A-D units also have substituents to increase solubility in appropriate solvents. Chloroform is by far the most commonly used solvent with APFO polymers. The first generation of APFOs has a relatively large band gap and is red. Later generations with lower band gaps have different colors and this is sometimes reflected in the name such as in APFO-GreenX, which is then of green color.

Experience shows that the influence of the fluorene part is limited, and in later generations of polymers it is replaced by other groups, which are no longer APFOs, but retains much of the chemistry.

A.1.1 APFO-3

APFO-3 is one of the first and most simple APFOs to be synthesized. A very weak D-A-D character gives the polymer a red color.

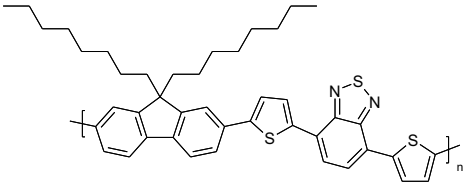

Figure A.1. APFO-3.

A.1.2 APFO-4

APFO-4 is very similar to APFO-3 with slightly longer side-chains (12 carbon instead of 8) as the only difference.

A.1.3 APFO-Green5

APFO-Green5 has a considerably more elaborate structure than APFO-3 and has a slightly stronger D-A-D character that gives the polymer a green color.

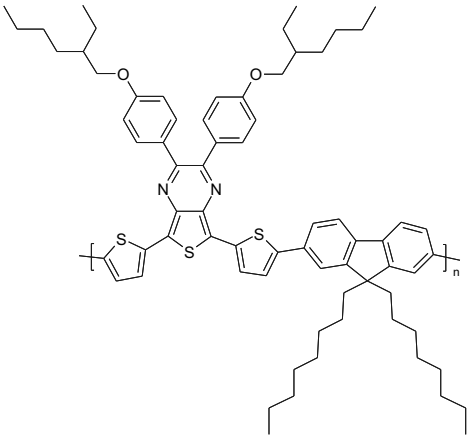

Figure A.2. APFO-Green5.

A.2 Fullerenes

Fullerenes are carbon balls of various sizes. The most common has 60 carbon (C60) atoms and is spherical. Larger balls, such as those with 70 carbon (C70), have a more elliptical circumference in one direction. As with polymers, fullerenes need to have substituents in order to be soluble.

A.2.1 PCBM60

[6,6]-phenyl-C61-butyric acid methylester (PCBM60) is one of the first substituted C60 to be synthesized and is still one of the best performers and most commonly used acceptors. PCBM60 is commercially available.

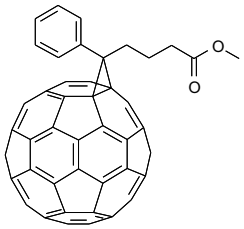

Figure A.3. PCBM60.

A.2.2 BTPF70

3'-(3,5-Bis-trifluoromethylphenyl)-1'-(4-nitrophenyl)pyrazolino[70]fullerene (BTPF70) is an alternative C70 molecule that has slightly different HOMO and LUMO levels compared to PCBM60.

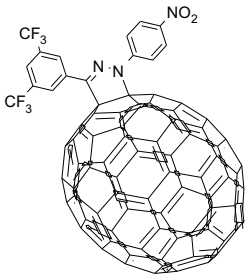

Figure A.4. BTPF70

A.3 PEDOT

Poly(3,4-ethylenedioxythiophene) (PEDOT) is, for a polymer, highly conductive in its doped state. It is commercially available in many forms, both solid and in a solvent as a dispersion. Dispersions of PEDOT doped with poly(styrenesulfonate) (PSS) have a conductivity on the order of $0.1 S/cm$ when used as is in thin films.

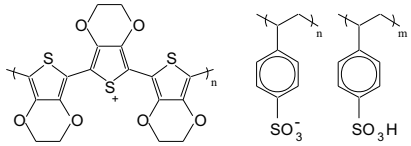

Figure A.5. PEDOT-PSS. PEDOT on the left is doped by PSS on the right.

List of Publications

[I] L. Mattias Andersson, and Olle Inganäs. Acceptor Influence on Hole Mobility in Fullerene Blends with Alternating Copolymers of Fluorene. *Applied Physics Letters*, 88:082103, 2006.

[II] L. Mattias Andersson, Fengling Zhang, and Olle Inganäs. Bipolar Transport Observed through Extraction Currents on Organic Photovoltaic Blend Materials. *Applied Physics Letters*, 89:142111, 2006.

[III] L. Mattias Andersson, and Olle Inganäs. Non-Equilibrium Effects on Electronic Transport in Organic Field Effect Transistors. *Organic Electronics*, 8:423, 2007.

[IV] L. Mattias Andersson, Fengling Zhang, and Olle Inganäs. Stoichiometry, Mobility, and Performance in Bulk Heterojunction Solar Cells. *Applied Physics Letters*, 91:071108, 2007.

[V] L. Mattias Andersson, Wojciech Osikowicz, Fredrik Jacobsson, Lars Lindgren, Mats R. Andersson, and Olle Inganäs. Intrinsic and Extrinsic Influences on the Temperature Dependence of Mobility in Conjugated Polymers. *In manuscript*.

[VI] Fengling Zhang, Wendimagegn Mammo, L. Mattias Andersson, Shimelis Admassie, Mats R. Andersson, and Olle Inganäs. Low Band-gap Alternating Fluorene Copolymer/Methanofullerene Heterojunctions in Efficient Near Infrared Polymer Solar Cells. *Advanced Materials*, 18:2169, 2006.

[VII] Abay Gadisa, L. Mattias Andersson, Fengling Zhang, Shimelis Admassie, Wendimagegn Mammo, Mats R. Andersson, and Olle Inganäs. A new Donor-Acceptor-Donor Polyfluorene Copolymer with Balanced Electron and Hole Mobility. *Advanced Functional Materials*, 2007. In press.

[VIII] Erik Perzon, Fengling Zhang, L. Mattias Andersson, Wendimagegn Mammo, Olle Inganäs and, Mats R. Andersson. A Conjugated Polymer for Near Infrared Optoelectronic Applications. *Advanced Materials*, 2007. In press.

[IX] Miaoxiang Chen, Xavier Crispin, Erik Perzon, Mats R. Andersson, Tönu Pullerits, L. Mattias Andersson, Olle Inganäs, and Magnus Berggren. High Carrier Mobility in Low Band Gap Polymer-Based Field-Effect Transistors. *Applied Physics Letters*, 87:252105, 2005.